学　位　論　文

Studies on the functional roles of biglycan in tumor microenvironment

（腫瘍微小環境における biglycan の役割に関する研究）

2021 年 9 月

北　海　道　大　学

リ　コン

Li Cong

学　位　論　文

Studies on the functional roles of biglycan in tumor microenvironment

(腫瘍微小環境における biglycan の役割に関する研究)

2021 年 9 月

北　海　道　大　学

リ　コン

Li Cong

List of Publications

1. **Li Cong**, Nako Maishi, Dorcas A. Annan, Marian F. Young, Hirofumi Morimoto, Masahiro Morimoto, Jin-Min Nam, Yasuhiro Hida and Kyoko Hida. Inhibition of stromal biglycan promotes normalization of the tumor microenvironment and enhances chemotherapeutic efficacy. *Breast Cancer Research*. (2021) 23:51

2. Dorcas A. Annan, Nako Maishi, Tomoyoshi Soga, Randa Dawood, **Cong Li**, Hiroshi Kikuchi, Takayuki Hojo, Masahiro Morimoto, Tetsuya Kitamura, Mohammad Towfik Alam, Kazuyuki Minowa, Nobuo Shinohara, Jin-Min Nam, Yasuhiro Hida and Kyoko Hida. Carbonic anhydrase 2 (CAII) supports tumor blood endothelial cell survival under lactic acidosis in the tumor microenvironment. *Cell Communication and Signaling.* (2019) 17:169.

3. Hirofumi Morimoto, Yasuhiro Hida, Nako Maishi, Hiroshi Nishihara, Yutaka Hatanaka, **Cong Li**, Yoshihiro Matsuno, Toru Nakamura, Satoshi Hirano and Kyoko Hida. Biglycan, tumor endothelial cell secreting proteoglycan, as possible biomarker for lung cancer. *Thorac Cancer*. (2021) 12:1347–1357.

List of Presentations

1. Li C, 間石奈湖, Annan DA, 樋田泰浩, 樋田京子: Inhibition of stromal biglycan normalizes tumor microenvironment and enhances chemotherapeutic efficacy, 第 28 回日本血管生物医学会学術集会, 2021.3.12（WEB 開催）

2. Li C, Maishi N, Annan DA, Young MF, Hida Y, Hida K: Inhibition of biglycan normalizes tumor blood vessels and potentiates tumor immune responses, ポスター, 第 6 回北海道大学部局横断シンポジウム“若手研究者による生命と物質の融合を目指して！”, 2020.10.19（WEB 開催）

3. Li C, Maishi N, Annan DA, Hida Y, Hida K: Inhibition of biglycan normalizes tumor blood vessels and potentiates tumor immune responses, 第 122 回北海道癌談話会, 2020.10.17（札幌）

4. Li C, Maishi N, Annan DA, Hida Y, Hida K: Stroma Biglycan deficiency normalizes tumor blood vessels and potentiates tumor immune responses, Oral, The 79th Annual Meeting og the Japanese Cancer Association, 2020.10.1-3, Hiroshima, Web Conference

5. Li C, Maishi N, Annan DA, Hida Y, Hida K: Biglycan deficiency normalizes tumor blood vessels and potentiates tumor immune responses, E-poster, The 21st International Vascular Biology Meeting (IVBM 2020), 2020.9.9-12, Seoul, Korea

6. Li Cong, Nako Maishi, Dorcas A. Annan, Marian F. Young, Yasuhiro Hida, Kyoko Hida: Biglycan promotes tumor angiogenesis, desmoplasia and potentiates tumor immune responses, 第 5 回北海道大学部局横断シンポジウム, 2019. 11. 5（札幌）

7. Li Cong, Maishi N., Dorcas A. Annan, Hida Y., Hida K.: Stromal biglycan promotes tumor angiogenesis and potentiates tumor immune responses, 第 79 回日本癌学会学術総会, 2019. 9. 27（京都）

8. Li Cong, 間石奈湖, Young Marian F, 森本浩史, 森本真弘, Annan Dorcas A., 樋田泰浩, 樋田京子: The involvement of stromal biglycan in tumor angiogenesis and metastasis, 第 51 回北海道病理談話会, 2018. 10. 13（札幌）

Summary

Background and Purpose:

Angiogenesis is required for tumor growth and metastasis. Tumor vasculature is structurally and functionally abnormal relative to normal vasculature. Tumor blood vessels are immature and leaky, and cannot sufficiently transport anticancer drugs and immune cells that attack cancer cells. In addition, tumor is excessively fibrotic, which is a barrier to the migration of immune cells leading to an insufficient response of immunotherapy and anticancer drug treatment. Normalization of tumor blood vessels benefits tumor microenvironment by promoting tumor blood flow, reducing tumor hypoxia and increasing drug delivery. Thus, normalization of tumor vasculature enhances the effects of anticancer drugs and immunotherapy. Although transient vessel normalization using bevacizumab has been shown in human cancers, sustained vessel normalization by deleting genes of interests is impossible in patients. Therefore, developing more effective strategies for cancer treatment is highly desirable.

The morphological abnormalities observed in tumor blood vessels compared with normal blood vessels raise the question of whether there are phenotypic differences at the molecular and functional levels between tumor endothelial cells (TECs) and normal endothelial cells (NECs). TECs differ from NECs in several aspects, such as gene expression profiles, proangiogenic properties, sensitivity to drugs, and responses to growth factors. Furthermore, TECs are cytogenetically abnormal. Previously we have found that biglycan, a proteoglycan in the extracellular matrix, is highly expressed in TECs. Biglycan is proteolytically cleaved from the ECM upon tissue stress or injury in a soluble form, thereby acting as a damage-associated molecular pattern (DAMP) protein. Biglycan secreted from TECs induces tumor angiogenesis and facilitates tumor metastasis. Furthermore, biglycan expressed tumor blood vessels in lung cancer patients are associated with a poor prognosis in our recent findings. The antitumor effect by targeting biglycan was expected, but the inhibitory effect in tumor mouse model was unknown. In the present study, we focused on the functional role of stromal biglycan in breast cancer microenvironment using biglycan-knockout (*Bgn* KO) mice, especially in tumor angiogenesis and immune responses. The therapeutic efficacy of targeting stromal biglycan combined with conventional chemotherapy in breast cancer was also investigated.

Materials and Methods:

By bioinformatics analysis, we compared and analyzed biglycan expression and patient prognosis in human breast cancer patients using TCGA database. E0771 murine breast cancer model was created using *Bgn* KO mice and wild-type mice. Tumor growth and metastasis were evaluated. The structure of tumor blood vessels was examined by immunostaining using tumor tissue specimens by comparing blood vessel density, the number of pericyte-covered blood vessels lectin-positive blood vessels and hypoxic regions. We also evaluated the number of CD8-positive T cell infiltrations by flow cytometry and immunostaining and cancer fibrosis by Picro Sirius Red staining. Furthermore, we analyzed the amount of drug delivery to cancer tissue via blood vessels and compared the therapeutic effects of the anticancer drug paclitaxel between *Bgn* KO and wild type tumors.

Results:

Breast cancer patients with high biglycan expression had shorter progression-free survival, suggesting that biglycan expression is a poor prognostic factor. Furthermore, biglycan expression was higher in the tumor stromal compartment compared to the epithelial compartment. Biglycan was positively associated with angiogenesis related genes PECAM1 and ANGPT2 in human breast cancer patients. Biglycan was highly expressed in tumor stroma from E0771 tumors, especially in tumor blood vessels. Knockout of biglycan in the stroma in E0771 tumor-bearing mice inhibited metastasis to the lung without affecting tumor growth. Histologically, *Bgn* KO was impaired tumor angiogenesis, the number of blood vessels covered with pericytes increased, and blood vessels were normalized by repressing tumor necrosis factor-α (TNF-α)/angiopoietin 2(Angpt2) signaling. TNF-α-enhanced Angpt2 expression is controlled by biglycan through activation of nuclear factor-κB (NF- κB) and extracellular signal-regulated kinase (ERK) via toll-like receptor (TLR) 2/4. Moreover, fibrosis was suppressed and CD8+ T-cell infiltration was increased in tumor-bearing *Bgn* KO mice. Furthermore, chemotherapy drug delivery and anti-tumor efficacy were improved *in vivo* in *Bgn* KO mice.

Discussion:

Biglycan has been extensively investigated in cancer cells. Biglycan has bidirectional roles modulating tumor growth and progression. However, the expression and function of stroma biglycan in tumor microenvironment required to be elucidated. By bioinformatics analysis,

biglycan was only expressed in tumor blood vessels of mouse breast cancers, and not in normal mammary gland tissue. Furthermore, co-expression analysis by cBioPortal showed that BGN was positively associated with PECAM1 and ANGPT2 expression in human breast cancers. Both PECAM1 and ANGPT2 genes are encoding the angiogenesis related molecules, which means that BGN is involved in regulating angiogenesis. In the current study, we found that stromal biglycan inhibition enhanced chemotherapeutic efficacy through normalization of the vasculature by downregulation of Angpt2 expression resulting in increased oxygen perfusion and the delivery of chemotherapy agents. To our knowledge, this is the first report demonstrating that stromal biglycan mediates the abnormality of the tumor vasculature, suggesting that biglycan may be regarded as a promising candidate to normalization of tumor vasculature in breast cancer.

Furthermore, biglycan depletion in stroma suppressed tumor fibrosis as well as downregulated collagen I expression. Furthermore, α -SMA + fibroblasts were fewer in biglycan depleted tumors. Biglycan may activate CAFs via upregulating α-SMA expression, thus enhancing fibrosis. Increasing ECM stiffness can enhance cancer progression and metastasis.

Thus, a novel target (biglycan) has been discovered to normalize the tumor microenvironment by normalization of tumor vasculature, suppressing cancer fibrosis and improvement immune cell recruitment. In addition, biglycan is expected to enhance the therapeutic effect of immunotherapy and anticancer drugs and reduce side effects. Normalization of blood vessels that carry drugs and suppression of fibrosis of cancer tissues are expected to lead to enhanced effects of anticancer drug treatment and immunotherapy. The therapeutic efficacy of targeting biglycan combined with immunotherapy will be needed to be discovered. To target biglycan in specific cells, biglycan conditional knock-out mice will be used in the future study. Research is also expected to establish the development of inhibitors targeting biglycan and effective administration methods.

Conclusion:

Our results showed that inhibition of biglycan enhances the effects of anticancer drugs and the effects of cancer immunity through normalization of the cancer microenvironment. Targeting stromal biglycan may yield a potent and superior anti-cancer effect in breast cancer.

List of Abbreviations

Bgn KO	biglycan-knockout
BSA	bovine serum albumin
DMFS	distant metastasis-free survival
DAMP	damaged-associated molecular pattern
EC	endothelial cell
ECM	extracellular matrix
ERK	extracellular signal-regulated kinase
FGF	fibroblast growth factor
HIF-1	hypoxia-inducible factor1
IFP	interstitial fluid pressure
IFP	interstitial fluid pressure
MAPK	mitogen-activated protein kinase
NF-κB	nuclear factor-κB
NECs	normal endothelial cells
PDGF-B	platelet-derived growth factor B
PI	propidium iodide
RT	room temperature
ROS	reactive oxygen species
SLRP	small leucine-rich proteoglycan
TGF-β	transforming growth factor beta
TECs	tumor endothelial cells
TLR	toll-like receptor
TNF-α	tumor necrosis factor alpha
TNBC	triple negative breast cancer
VEGF	vascular endothelial growth factor
WT	wild type

Introduction

Angiogenesis is required for invasive tumor growth and metastasis and constitutes an important point in the control of cancer progression (Folkman, 2002). Tumor blood vessels are structurally abnormal relative to normal blood vessels (Nagy et al., 2009). Most of tumor blood vessels are lack of pericytes and vascular smooth muscle cells , they are dilated and convoluted, and lack of a complete basement membrane (Papetti and Herman, 2002). Functionally, tumor blood vessels are highly permeable and leaky blood vessels (Nagy et al., 2006). The abnormality of tumor vasculature impairs blood perfusion and oxygenation, resulting in hypoxia and acidosis, and thus promoting tumor growth and progression (Jain et al., 2007). Furthermore, the leakiness of tumor blood vessels results in spontaneous hemorrhages and elevated interstitial fluid pressure (IFP) (Jain et al., 2007). Hypoperfusion, hypoxia, and high IFP impede the functions of immune cells in tumors, in addition to impeding the transport of therapeutic agents (Stylianopoulos et al., 2018). As a result, abnormal tumor vasculature can promote drug resistance and hinder anti-cancer activity (Kikuchi et al., 2020).

Tumor angiogenesis is driven largely by hypoxia which is a hallmark of the tumor microenvironment (Semenza, 2010). Hypoxia leads directly to the production of proangiogenic factors such as vascular endothelial growth factor (VEGF) and fibroblast growth factor (FGF)(Semenza, 2010). VEGF and other proangiogenic factors in tumor microenvironment drives continual tumor angiogenesis and the establishment of an abnormal blood vessel network (Carmeliet and Jain, 2011a). Proangiogenic factors also weaken of VE-Cadherin-mediated endothelial cell (EC) junctions and EC migration (Hashizume et al., 2000). Furthermore, proangiogenic factors regulate molecules mediating pericyte–EC interaction, including platelet-derived growth factor-B (PDGF-B), Angiopoietin 1, transforming growth factor-b (TGF-b), and sphingosine-1-phosphate (S1P) (Goel et al., 2012). Thus, pericytes and vascular smooth muscle cells are often only loosely attached to ECs and are reduced in number in tumor tissues(Goel et al., 2012).

Female breast cancer is the most commonly diagnosed cancer, with an estimated 2.3 million new cases (11.7%) worldwide in 2020 (Sung et al., 2021). Anti-angiogenic therapy has been considered as a promising treatment strategy for breast cancer (Miller et al., 2007). Bevacizumab, a neutralizing

antibody against VEGF, mediates anti-tumor effects by blocking tumor blood supply (Xu et al., 2009). Bevacizumab received FDA approval for metastatic breast cancer in 2008. However, other trials found no significant effect on prolonging progression-free survival using Bevacizumab resulting in withdrawal of FDA approval (Luck et al., 2015; Welt et al., 2016). Bevacizumab induces tumor hypoxia by excessively vessel pruning and forming dysfunctional vessels, and eventually leads to insufficient efficacy and the development of resistance (Itatani et al., 2018). Thus, alternative strategies to modulate abnormal tumor vasculature in breast cancer are still needed.

Vascular normalization is regarded as a therapeutic strategy for tumor (Goel et al., 2012). Vascular normalization is stated that direct or indirect antiangiogenic therapy tips the imbalance between pro- and antiangiogenic factors back toward equilibrium (Jain, 2005). As a result, vessel structure and function become more normal: vessels are more mature with enhanced pericyte coverage, blood flow is more homogeneous, vessel permeability and hypoxia are reduced, and importantly the delivery of systemically administered anticancer therapies into tumors is more uniform (Goel et al., 2012). Normalization of tumor vasculature by increased pericyte recruitment and enhanced vessel functions using bevacizumab has been shown in cancer patients (Gerstner et al., 2020; Tolaney et al., 2015; Ueda et al., 2017). Although transient vessel normalization using bevacizumab has been shown in human cancers, sustained vessel normalization by deleting genes of interests is impossible in patients (Fu et al., 2020; Rivera and Bergers, 2015), therefore developing more effective strategies for cancer treatment is highly desirable.

The morphological abnormalities observed in tumor blood vessels compared with normal blood vessels raise the question of whether there are phenotypic differences at the molecular and functional levels between tumor endothelial cells (TECs) and normal endothelial cells (NECs) (Hida et al., 2016). Tumor endothelial cells (TECs) differ from normal endothelial cells (NECs) in several aspects, such as gene expression profiles (Hida et al., 2008), proangiogenic properties (Matsuda et al., 2010), sensitivity to drugs (Ohga et al., 2009), and responses to growth factors(Amin et al., 2006). Furthermore, TECs are cytogenetically abnormal (Hida et al., 2004). In our lab, by comparing the gene expression profiles of TECs and NECs, we have previously shown that biglycan gene expression levels are significantly elevated in isolated TECs (Yamamoto et al., 2012).

Biglycan is a small leucine-rich proteoglycan (SLRP), consisting of a 42-kDa core protein and chondroitin sulfate/dermatan sulfate side chains (Iozzo, 1999). Biglycan is involved in the migration of lung fibroblasts, the inflammatory response in renal macrophages, and abnormal collagen fibril morphology in bones (Ameye et al., 2002; Poluzzi et al., 2019; Tufvesson and Westergren-Thorsson, 2003). Under physiological conditions, biglycan is sequestered in the extracellular matrix (ECM). Biglycan is proteolytically cleaved from the ECM upon tissue stress or injury in a soluble form, thereby acting as a damage-associated molecular pattern (DAMP) protein (Moreth et al., 2010). During renal inflammatory diseases, biglycan interacts with Toll-like receptor (TLR) 2 and 4 on macrophages and activates mitogen-activated protein kinase (MAPK) p38, extracellular signal-regulated kinase (ERK), and nuclear factor-κB (NF- κB) resulting in the production of several cytokines and chemokines such as tumor necrosis factor alpha (TNF-a), chemokine (C–C motif) ligand (CCL)2, CCL5, chemokine (C-X-C motif) ligand (CXCL) 2, and CXCL13 (Hsieh et al., 2014; Moreth et al., 2014; Roedig et al., 2019) (Figure I 1). Biglycan is also involved in collagen fibril assembly and soluble biglycan acts as a fibrosis marker for in patients with chronic hepatitis B (Ciftciler et al., 2017). In endothelial cells, biglycan enhanced the interaction between transcription factor HIF1a and VEGF promoter (Hu et al., 2016) (Figure I 2). Biglycan intensifies ALK5- Smad 2/3 signaling resulting downregulation of syndecan 4 (Hara et al., 2017) (Figure I 2). It is suggested that biglycan may be involved in disturbing normal structure of ECM in vascular endothelial monolayer. Biglycan overexpression in smooth muscle cells enhances proliferation and migration of smooth muscle cells with an increase expression of CDK2 and decrease expression of p27 (Shimizu-Hirota et al., 2004) (Figure I 2).

Biglycan has also been detected in several types of human cancer cells, such as endometrial cancer, bladder cancer and pancreatic adenocarcinoma (Aprile et al., 2013; Liu et al., 2014; Schulz et al., 2019). Functionally, biglycan expressed in cancer cells is involved in tumor growth and progression, depending on tumor types. Silencing biglycan in bladder cancer cells resulted in enhanced tumor cell proliferation which indicates that biglycan acts as a tumor suppressor in tumor growth (Niedworok et al., 2013). In contrast, biglycan overexpression in gastric cancer cells enhances the invasive capacity of cancer cells by activating the FAK signaling pathway (Hu et al., 2014). Similarly, biglycan overexpression in colon cancer cells promotes tumor angiogenesis and tumor growth through upregulating the levels of VEGFA via ERK signaling pathway (Xing et al., 2015).

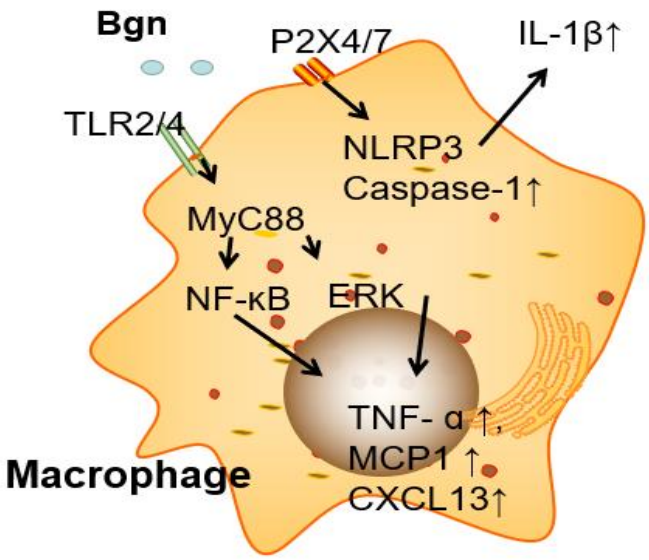

Figure I 1. Biglycan-mediated proinflammatory signaling in macrophages (Figure information cited from Hsieh et al., 2014; Moreth et al., 2014; Roedig et al., 2019).

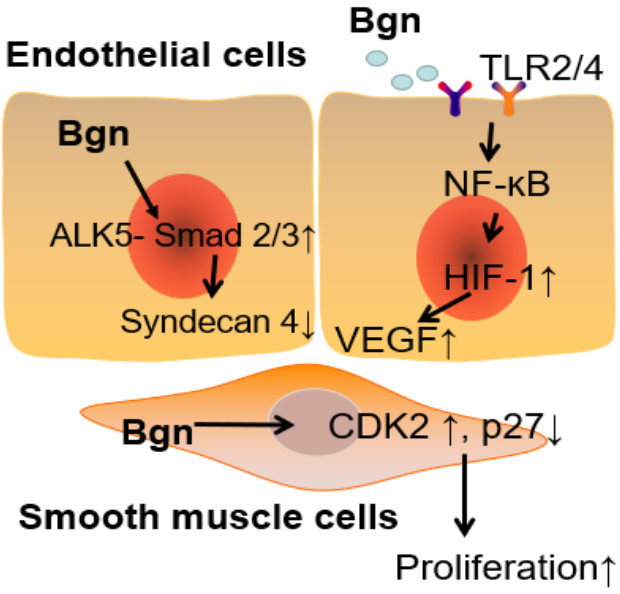

Figure I 2. Biglycan signaling in endothelial cells and smooth muscle cells (Figure information cited from Hu et al., 2016, Hara et al., 2017, Shimizu-Hirota et al., 2004).

However, the role of biglycan in tumor stroma is still needed to be clarified. In our previous study, biglycan upregulated in TECs compared to in NECs, suggesting the possible a TEC marker (Yamamoto et al., 2012). Biglycan secreted from TECs can induce pro-angiogenic effects in an autocrine manner (Yamamoto et al., 2012). In addition, TECs derived from high metastasis tumor express higher level of biglycan expression compared to TECs derived from low metastasis tumor and NECs (Maishi et al., 2016). Biglycan can be only detected in TECs from highly metastatic tumor conditioned medium. Furthermore, biglycan secreted from TECs, binding to toll-like receptor (TLR)2 or TLR4 on tumor cells, promotes tumor cell intravasation and metastasis through activation of NF-κB and ERK signaling (Maishi et al., 2016). The antitumor effect by targeting biglycan was expected, but the inhibitory effect in tumor model was unknown. In the present study, we focused on the functional role of stromal biglycan in breast cancer microenvironment using biglycan-knockout (*Bgn* KO) mice, especially in tumor angiogenesis and immune responses. The therapeutic efficacy of targeting stromal biglycan combined with conventional chemotherapy in breast cancer was also investigated.

Methods

Bioinformatic analysis

We compared biglycan mRNA levels in human breast cancers (n = 389) and normal mammary gland (n = 61), 14 patient-matched tumor epithelium and tumor-associated stroma specimen using Oncomine (https://www.oncomine.com/). The relationship between the prognostic significances and biglycan mRNA and protein levels in human breast cancers were evaluated using the Kaplan-Meier plotter (http://kmplot.com/analysis/). Co-expression of biglycan and angiogenesis-related genes (PECAM1 and ANGPT2), fibrosis-related gene (COL1A1) was determined using the cBioPortal database (https://www.cbioportal.org/).

Cell lines and culture conditions

MS1 cells (mouse immortalized islet-derived normal endothelial cells) were obtained from American Type Culture Collection (Manassas, VA) and cultured in Dulbecco's Minimum Essential Medium (DMEM, Sigma–Aldrich, St Louis, MO, USA) supplemented with 10% heat-inactivated fetal bovine serum (FBS) and 1% penicillin/streptomycin antibiotics (Sigma-Aldrich). E0771 cells were purchased from CH3 BioSystems and cultured in Roswell Park Memorial Institute (RPMI) 1640 medium (Sigma-Aldrich) supplemented with 10 mM HEPES and 10% FBS. RAW264.7 cells were purchased from DS Pharma Biomedical and cultured in DMEM with 10% FBS. Dermal endothelial cells from C57BL/6 mice were obtained from Cell Biologics and cultured in EGM-2MV microvascular endothelial cell growth medium (Lonza, Basel, Switzerland). NIH3T3 cells obtained from American Type Culture Collection (ATCC) were cultured in DMEM with 10% FBS. All cells were cultured at 37°C in a humidified atmosphere containing 5% CO_2. The absence of *Mycoplasma pulmonis* was confirmed by polymerase chain reaction (PCR).

In *vitro* cell proliferation assay

The proliferation of E0771 tumor cells under the effect of biglycan was measured by the MTS [3-(4,5-dimethylthiazol-2-yl)-5-(3-carboxymethoxyphenyl)-2-(4-sulfophenyl)-2H-tetrazolium] assay (CellTiter

96 Non-Radioactive Cell Proliferation Assay; Promega, Madison, WI), which monitors the number of viable cells. Cultured cells were seeded at 1 × 10^3 cells per well in 96-well flat-bottomed plates containing RPMI 1640 medium with different concentrations of recombinant biglycan (Genway, GWB-ATG116). The cells were recorded the absorbance at 490nm with a 96-well plate reader every 24 hours.

Mouse tumor xenograft model and drug administration

All animal experiments were approved by the local animal research authority, and the protocols for animal care were in accordance with the institutional guidelines Hokkaido University (Code of the conduct for animal research: 18-0050). Wild type (WT) C57BL/6 mice (female, 7-8 weeks old, 17-20g) were purchased from CLEA Japan (Tokyo, Japan). *Bgn* KO C57BL/6 mice (female, 7-9 weeks old, 18-20g) were used in this study. *Bgn* KO C57BL/6 mice were established by Marian F. Young (National Institutes of Health, USA) (Xu et al., 1998). Bgn-deficient mice were originally generated by using homologous recombination in embryonic stem cells. Biglycan was disrupted by inserting the PGK-neo cassette from the pPNT vector into exon 2 at the Tth111I site. The genotype of Bgn KO mice was determined by a PCR–based assay using the combination of a primer containing the PGK promoter sequences (5'-tggatgtggaatgtgtgcgagg-3') of the targeted allele along with a forward primer corresponding to the 5'-end of exon two (5'-caggaacattgaccatg-3') and a reverse primer corresponding to the 3'-end of exon two (5'-gaaaggacacatggcactgaag-3')(Xu et al., 1998). Biglycan was disrupted throughout the whole cells of the body. E0771 cells were transfected with lentiviral vectors encoding the tdTomato and luciferase genes as previously described (Maishi et al., 2016).The conducts of gene recombination and transfer have been approved by the Hokkaido University (Code: 2014-031). tdTomato/luc2-expressing E0771 cells (1 x10^6 cells) suspended in an equal volume of Hank's balanced salt solution (HBSS) and Matrigel (Corning, 356231) were orthotopically implanted into the left fourth mammary gland of WT and *Bgn* KO mice (5 mice per group). Tumor volumes were measured with a caliper every 3 or 4 days and calculated using the formula: volume (V) = largest dimension × smallest dimension^2 × 0.5. For histological analysis of tumors, mice were sacrificed 24 days after implantation. Lungs and left inguinal lymph nodes were analyzed for tumor metastasis by *ex vivo* bioluminescence imaging using the IVIS Spectrum system (Caliper Life Science). To evaluate the efficacy of *Bgn* KO on chemotherapy, mice were randomly assigned to 4 groups (4 or 5 mice per group) after tumor

formation (7 days after tumor cell inoculation), and treated with paclitaxel (PTX, Taxol, EnZo, BML0T104) (2 mg/kg) or DMSO as a control via intraperitoneal (i.p.) injection every 3 days, for a total of 6 injections (Figure M 1). After 22 days, mice were sacrificed via cervical dislocation after isoflurane anesthesia. Tumor tissues, lungs, and left inguinal lymph nodes were dissected. The IVIS imaging system was used to detect metastasis in lungs and lymph nodes.

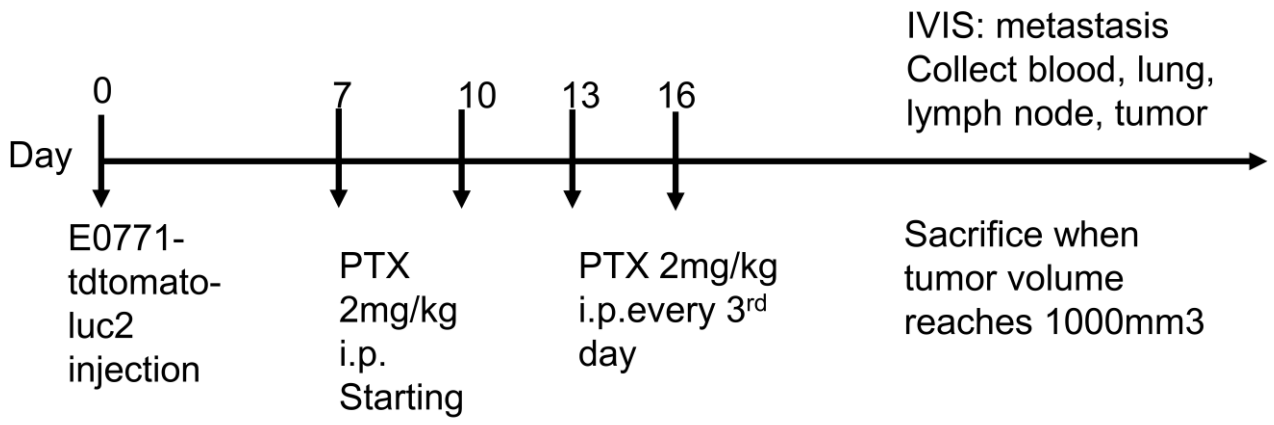

Figure M 1. Administration of paclitaxel in WT and *Bgn* KO mice

Isolation of TECs

Tumor endothelial cells were isolated from E0771 breast cancer xenografts in C57BL/6 mice (n =10, female, 7-8 weeks old, CLEA Japan). E0771 cells were orthotopically injected into the 4th left mammary glands of the mice. When E0771 tumors reached ∼1 cm in diameter, E0771 tumors grown in C57BL/6 mice were dissected and minced. Tumor tissues were subjected to digestion with collagenase II and DNase I. Blood cells were removed by lysis buffer (BD Pharm Lyse, 555899), and cell suspensions were filtered. TECs were sorted a magnetic cell sorting system (MACS, Miltenyi Biotec, Tokyo, Japan) with anti-mouse CD31 microbeads. To improve the purity of TECs, isolated cells were preincubated with mouse FcR blocking buffer (Miltenyi Biotec, 130-092-575) to blocking of the binding of antibodies to the Fc receptor of mouse Fc receptor–expressing cells, e.g., monocytes and macrophages, then incubated with FITC-CD45 anti-mouse antibody (Biolegend, 103107) and Alexa Fluor 647 -CD31 anti-mouse antibody (Biolegend, 102416). Propidium iodide (PI) was used to exclude dead cells. CD45-/CD31+ cells were gated and sorted using a FACS Aria II (BD Biosciences). CD45-/CD31+ cells were plated onto 1.5% gelatin-coated culture plates and maintained in EGM-2MV

medium (Lonza, Basel, Switzerland) with 15% FBS. After subculture for ~3 weeks, the isolated ECs were purified by a second round of purification using APC-anti-CD31 antibody. Purified ECs were characterized by FACS and PCR. Isolated cell monolayers were detached with 1% trypsin-EDTA and incubated with APC anti-Mouse CD45 (Biolegend, 103112), Alexa Flour 647 anti-mouse CD31 (Biolegend, 102416), Alexa Fluor 488 anti-mouse CD105 (Biolegend, 120406) and Fluorescein Griffonia Simplicifolia Lectin Isolectin B4 (Vector Laboratories, FL-1201) for 30 minutes at 4°C. A minimum of 10,000 cells per samples were analyzed on a FACS Aria II (BD Biosciences). Representative data was analyzed using FlowJo V10 software (Tree Star Inc.). All of the PCR reactions were run for 32 cycles using mouse-specific primers for endothelial cell markers CD31, CD144, CD105, monocyte marker CD11b and hematopoietic cell marker CD45. The primers of these markers were listed in Table 1. All purified ECs were cultured in EGM-2MV and were used between passages 12 and 20. The scheme of the TEC isolation procedure edited by BioRender (https://app.biorender.com/) was shown as below (Figure M 2).

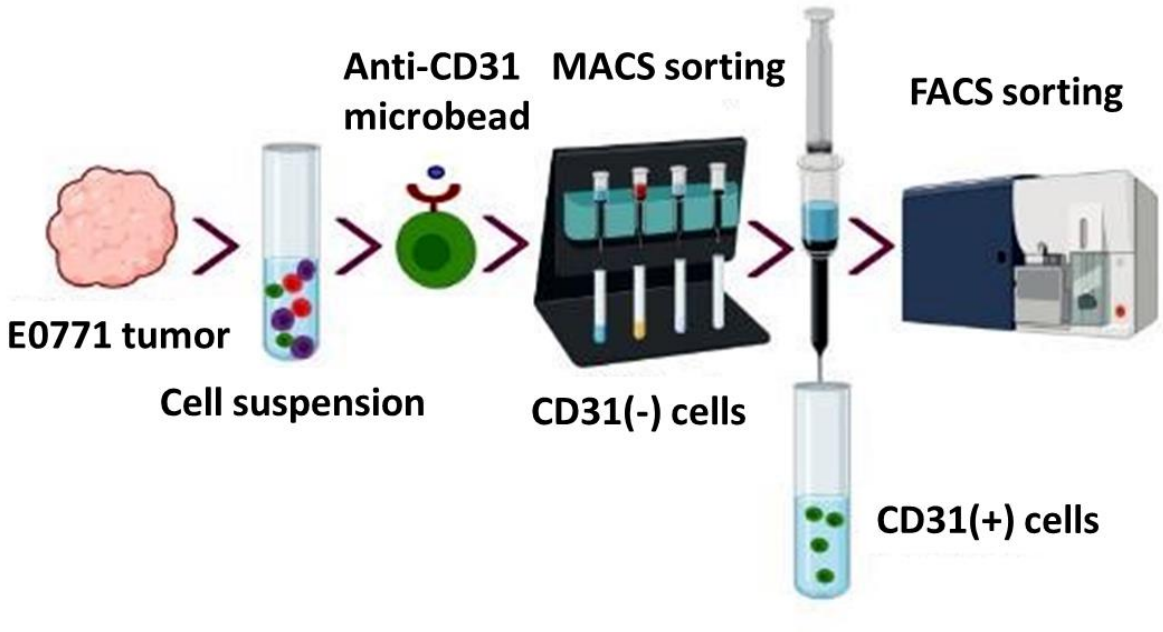

Figure M 2. The procedure of TEC isolation

Histological analysis

Tumor tissues were dissected from euthanized mice and half of the tumor tissues were processed for formalin-fixed and paraffin-embedded (FFPE) sections. After deparaffinization and rehydration, FFPE sections (4 μm) were brought to a boil in 10 mM Sodium Citrate buffer (pH 6.0) and then maintain at a sub-boiling temperature for 30 minutes for antigen retravel. To block endogenous peroxidase activity, quench the tissue sections with 3.0% hydrogen peroxide (H_2O_2) in DDW for 10 minutes. FFPE sections were blocked with 5% goat serum in 1x PBS and stained with anti-mouse CD31 antibody (Abcam, ab28364) and counterstained with hematoxylin. Another half of tumor tissues were embedded in OCT compound and immediately immersed in liquid nitrogen, Frozen tissue samples were cut into 10-μm sections using a cryostat (Leica CM3050S, Leica Biosystems, Wetxlar, Germany). Sections were fixed in 100% ice-cold acetone for 30 min and permeabilized with 0.1% Triton X-100 in PBS at room temperature (RT) for 15 min. Sections were then blocked in PBS containing 5% bovine serum albumin (BSA) or 5% goat serum and 0.05% Triton X-100. Frozen tumor tissues were double stained using Alexa Fluor 647-conjugated anti-mouse CD31 antibody (Biolegend, 102416) and anti-biglycan (Kerafast, LF-159) antibodies to determine the co-localization of CD31 and biglycan in ECs. Pericyte-covered tumor blood vessels in frozen sections were visualized by the co-staining of rat anti-mouse CD31 (BD Pharmingen, 553370) and rabbit anti-mouse α-SMA (Abcam, ab5694) followed by Alexa Fluor 647-conjugated goat anti-rat IgG (Biolegend, 405416) and Alexa Fluor 488-conjugated goat anti-rabbit IgG (Invitrogen, 11034) for 2 h at room temperature. To detect hypoxia in tumors, frozen sections were stained with an anti-glucose transporter Glut1 antibody (Abcam, ab115730) followed by Alexa Fluor 647-conjugated goat anti-rabbit secondary antibody (Invitrogen, 21244). Frozen sections were counterstained with 4,6-diamidino-2-phenylindole (DAPI; Dojin), and images were obtained using a BZ-X810 microscope equipped with BZ-X800 Analyzer software (Keyence Corporation, Itasca, IL, USA). The area of CD31+ or Glut1+ staining was quantified using ImageJ software (NIH), and the percentage of CD31+ or Glut1+ area was calculated as a percentage of the positive area to the total area. The area of pericyte-covered tumor blood vessels was calculated by the ratio of the number of blood vessels co-stained with α-SMA and CD31 to the total number of CD31-positive blood vessels. Collagen accumulation was evaluated by Picro Sirius Red Stain Kit (Abcam, ab150681). 5 fields per tumor were quantified and values were averaged to obtain one value for each tumor. Each group consisted of 4 or 5 mice.

Immunocytochemistry

MS1 cells and E0771-TECs were cultured on cover slips in 6-well plates. Cells were fixed in 4%PFA for 15 min and then washed with PBS for 10 min. TECs were incubated with primary antibody rat anti-mouse CD31 (BD Pharmingen, 553370) for 16 h at 4 °C followed by Alexa Fluor 647-conjugated goat anti-rat IgG (Biolegend, 405416) for 2 h at room temperature. Immunoreactivity was visualized using a DAKO ENVISION Kit/HRP (DAB) (DAKO). Representative images were obtained using a BZ-X810 microscope equipped with BZ-X800 Analyzer software (Keyence Corporation, Itasca, IL, USA).

Assessment of perfused blood vessels

Doxorubicin (15 mg/kg, Sigma) was injected into the tail vein of E0771 tumor-bearing mice. FITC-lectin (2 mg/kg, Vector Laboratories) was intravenously injected via tail vein 4 h after doxorubicin injection. Tumors were extracted 5 min after injection and embedded in OCT compound, immediately immersed in liquid nitrogen, and cut into sections (10μm thick) using a cryotome. These frozen sections were stained with Alexa Fluor 488-conjugated anti-mouse CD31 antibody (Biolegend, 12514) or Alexa Fluor 647-conjugated anti-mouse CD31 antibody (Biolegend, 102416). The area of lectin- or doxorubicin-positive staining was determined using ImageJ software.

RNA isolation, reverse transcription PCR and quantitative real-time PCR

RNA from cells and tissues was isolated using the ReliaPrep RNA tissues miniprep system (Promega) and the RNeasy Micro kit (Qiagen), respectively. Total RNA was isolated from ECs using the RNeasy Micro kit (Qiagen) using the RNase-free DNase Set (Qiagen). RNA was quantified using spectrophotometry. Total RNA was then used for performing first-strand complementary DNA synthesis by using the ReverTra-Plus (Toyobo, Osaka, Japan). cDNA was amplified by PCR. The PCR protocol was as follows: Activation of polymerase: 95°C 1min; Thermal cycling: 40 cycles; Denaturation: 95°C, 15s; Annealing: 60°C, 15s; Initial extension: 72°C, 30s; Extension: 72°C, 3min; Storage: 4°C, as necessary. PCR products were visualized by ethidium bromide staining. Real-time PCR was conducted using the SYBR Green Realtime PCR Master Mix Plus (Toyobo). Quantitative real-time RT-PCR was performed using SoFast EvaGreen Supermix (Bio-Rad). Cycling conditions were set based on CFX Manager (Bio-Rad). mRNA expression levels were normalized to those of

Gapdh or *Actb* and analyzed using the delta-delta-Ct method. The primers used in this study are listed in Table 1.

Table 1. List of primers for PCR analysis

Genes	Sequences
Bgn	Forward 5'-AACTCACTGCCCCACCACAGCTTC-3'
	Reverse 5'-GCGGTGGCAGTGTGCTCTATCCATC-3'
Angpt2	Forward 5'-ACTCACCACCAGTGGCATCTAC-3'
	Reverse 5'- TCTCGGTGTTGGATGACTGTCC-3'
Tnf	Forward 5'-AAGCAAGCAGCCAACCAGGCAG-3'
	Reverse 5'-CGTCGCGGATCATGCTTTCTGTGC-3'
Col1a1	Forward 5'-GAGCGGAGAGTACTGGATCG-3'
	Reverse 5'-GTTCGGGCTGATGTACCAGT-3'
Cd4	Forward 5’- CAGGTCTCGCTTCAGTTTGCTG-3’
	Reverse 5'- GCTGAGCCACTTTCATCACCAC-3’
Klrb1c	Forward 5’- TTAGAGTGCCCACAAGACTGGC-3’
	Reverse 5’- TCAGCTTGACCTTCCTCCCAAG-3’
Cd27	Forward 5’- GCTGCAGGCATTGTAACTCTGG-3’
	Reverse 5’- TCTGTGCCATGAGGTAAGTGGG-3’
Adgre1	Forward 5’- TACAAGTGTCTCCCTCGTGCTG-3’
	Reverse 5’- TTCATCTTGTCCCCTCTGGCTG-3’
Cd8	Forward 5’-AGCCCCAGAGACCAGAAGATTG-3’

	Reverse 5'-CATTTGCAAACACGCTTTCGGC-3’
Hif1a	Forward 5’-AAACACTCCTAACTTTTCCCAGCC-3’
	Reverse 5’-TGGGATATAGGGAGCCAGCATC-3’
Slc2a1	Forward 5’-GAGTGACGATCTGAGCTACGGG-3’
	Reverse 5’-GAACGGACGCGCTGTAACTATG-3’
Acta2	Forward 5’-TTCCTTCGTGACTACTGCCGAG-3’
	Reverse 5’-ATAGGTGGTTTCGTGGATGCCC-3’
Gapdh	Forward 5'-CACTGAGCATCTCCCTCACA-3'
	Reverse 5'-GTGGGTGCAGCGAACTTTAT-3'
Actb	Forward 5'-TTTGCAGCTCCTTCGTTGCCGG-3'
	Reverse 5'-TTTGCACATGCCGGAGCCGTTG-3'
Pecam1	Forward 5'-TACAGTGGACACTACACCTG-3'
	Reverse 5'-GACTGGAGGAGAACTCTAAC-3'
Cd105	Forward 5′-CTTCCAAGGACAGCCAAGAG-3′
	Reverse 5′-GGGTCATCCAGTGCTGCTAT-3′
Cd144	Forward 5’-CAGCACTTCAGGCAAAAACA-3′
	Reverse 5’-TTCTGGTTTTCTGGCAGCTT-3′
Cd11b	Forward 5′-CCAAGAAAGTAGCAAGGAGTGTG-3'
	Reverse 5'-AGGGTCTAAGCCAGGTCATAAG-3'
Cd45	Forward 5′-CCTCAAACTTCGACGGAGAG-3′
	Reverse 5′-CACTTGCACCATCAGACACC-3′

ELISA

Biglycan concentration in mouse plasma was determined using a sandwich enzyme immunoassay by an ELISA kit for mouse biglycan (Cloud-clone Corp. SEJ226Mu). TNF-α concentration in mouse plasma was determined using a sandwich enzyme immunoassay by a mouse TNF-α Quantikine ELISA kit (R&D systems, MTA00B) according to the manufacturer's instructions. Absorbance was detected using a microplate reader (Promega GloMax Multi Detection System, Promega) at 450 nm.

Stimulation of cells with recombinant protein

E0771 cells were cultured in serum-free medium for 24 h before treatment with 5μg/ml recombinant biglycan (Genway, GWB-ATG116) in serum-free RPMI medium. After incubation for 6 h with recombinant biglycan protein, RNA was isolated. E0771 cell were pretreated with anti-TLR2 (1μg/ml, Biolegend, #246294) or TLR4 (10μg/ml, Biolegend, #117608) antibody for 2 h. E0771 cells were then treated with serum-free RPMI media containing 5μg/ml biglycan for 6 h before RNA was extracted. E0771 cell were pretreated with NF-κB inhibitor BAY11-7082 (10μM, Calbiochem) or MEK inhibitor U1026 (20μM, CST) for 1 h. E0771 cells were then treated with serum-free RPMI media containing 5 g/ml biglycan for 6 h before RNA was extracted. MS1 cells were kept in serum-free medium for 24 h before treatment with 1 g/ml TNF-α (Peprotech, 300-01A) in serum-free DMEM medium. After incubation for 6 h with recombinant biglycan protein, RNA was isolated. NIH3T3 cells were cultured in serum-free DMEM for 24 h before treatment with 5μg/ml recombinant biglycan in serum-free DMEM medium. After incubation for 6 h with recombinant biglycan protein, RNA was isolated.

Biglycan knockdown using siRNA

Biglycan siRNA (5'-UAGAGGUGCUGGAGGCCUUUFAAGU-3', 5′ -ACUUCAAAGGCCUCCAGCACCUCUA-3′) was transfected into E0771-TECs using Lipofectamine RNAi MAX Transfection Reagent (Invitrogen, Carlsbad, CA, USA) according to the manufacturer's instructions. Control siRNA (Invitrogen, Carlsbad, CA, USA) was used as a negative control.

Cell preparation and flow cytometry

To detect TLR2 and TLR4 expression in E0771 cells and MS1 cells, after E0771 cells or MS1 cells were detached with 0.5% trypsin–EDTA, all cells were incubated with PE-conjugated anti-mouse CD284 (Biolegend, 117605) and Alexa Fluor 488-conjugated anti-mouse CD282 (Biolegend, 121807) for 30 min at 4 °C. The cells were analyzed on a a FACS Aria II (BD Biosciences). Representative data was analyzed using FlowJo V10 software (Tree Star Inc.). To analyze CD8+ T cell infiltration in tumor tissues, E0771 tumors from WT and *Bgn* KO mice were dissected and digested with collagenase II and DNase I. Single-cell suspensions were stained with FITC-conjugated anti-CD45 antibody (Biolegend, 103115) and APC-conjugated anti-CD8a antibody (Biolegend, 100711). CD45+CD8+ T cells were analyzed using a FACS Aria II. Data was analyzed using FlowJo V10 software (Tree Star Inc.).

Statistical analysis

All data are expressed as means ± standard deviation (SD) of three independent experiments performed in triplicate. A two-sided Student's t-test followed by Wilcoxon rank test was used for comparison between two groups. Comparisons between multiple groups were made using One-way ANOVA, followed by a Tukey-Kramer test. One-way ANOVA and T tests were analyzed using IBM SPSS software. p-values < 0.05 were considered significant. *$p < 0.05$, **$p < 0.01$, ***$p < 0.001$. NS, not significant.

Results

Biglycan is highly expressed in tumor stroma, associated with prognosis and angiogenesis-related genes in human breast cancer.

To determine the relationship between biglycan and clinical significances, we first evaluated the expression levels of biglycan in human normal mammary glands and in human breast cancer tissues using the Oncomine database (https://www.oncomine.com/). Biglycan was upregulated in human breast cancers (n =389) compared to human normal mammary glands (n =61) (Fig. 1a). Furthermore, biglycan expression was higher in the tumor stroma compartment compared to the tumor epithelial compartment of human breast cancer tissues (n =14) (Fig. 1b). These results indicated that biglycan is upregulated in breast cancer, especially in tumor stroma. Next, we discovered the relationship between biglycan expression and prognosis of breast cancer patients using Kaplan-Meier Plotter database (http://kmplot.com/analysis/). Breast cancer patients with higher mRNA and protein expression of biglycan had worse distant metastasis-free survival (DMFS) of breast cancer patients (Fig. 1c, d). These results suggested that biglycan expression is negatively associated with the survival of breast cancer patients. Biglycan has been reported to be involved in cell migration and tube formation of ECs (Yamamoto et al., 2012). To determine the effect of biglycan on angiogenesis in human cancers, we analyzed the correlation between biglycan and angiogenesis-related gene expression in human breast cancers using the cBioPortal database (https://www.cbioportal.org/). Platelet endothelial cell adhesion molecule (PECAM)-1 has been shown to facilitate the interaction of endothelial cells and play a role in angiogenesis (Cao et al., 2002). Angiopoietin 2 (ANGPT2) destabilizes blood vessels by inducing detachment of pericytes from the endothelial cells (Schrimpf et al., 2014). Pearson's correlation coefficients showed that biglycan mRNA expression was positively correlated with both PECAM1(Spearman’s correlation =0.45) and ANGPT2 (Spearman’s correlation = 0.4) levels in human breast cancers (Fig. 1e, f). Taken together, these results suggest that biglycan may be involved in tumor angiogenesis and destabilization of tumor blood vessels in human breast cancers.

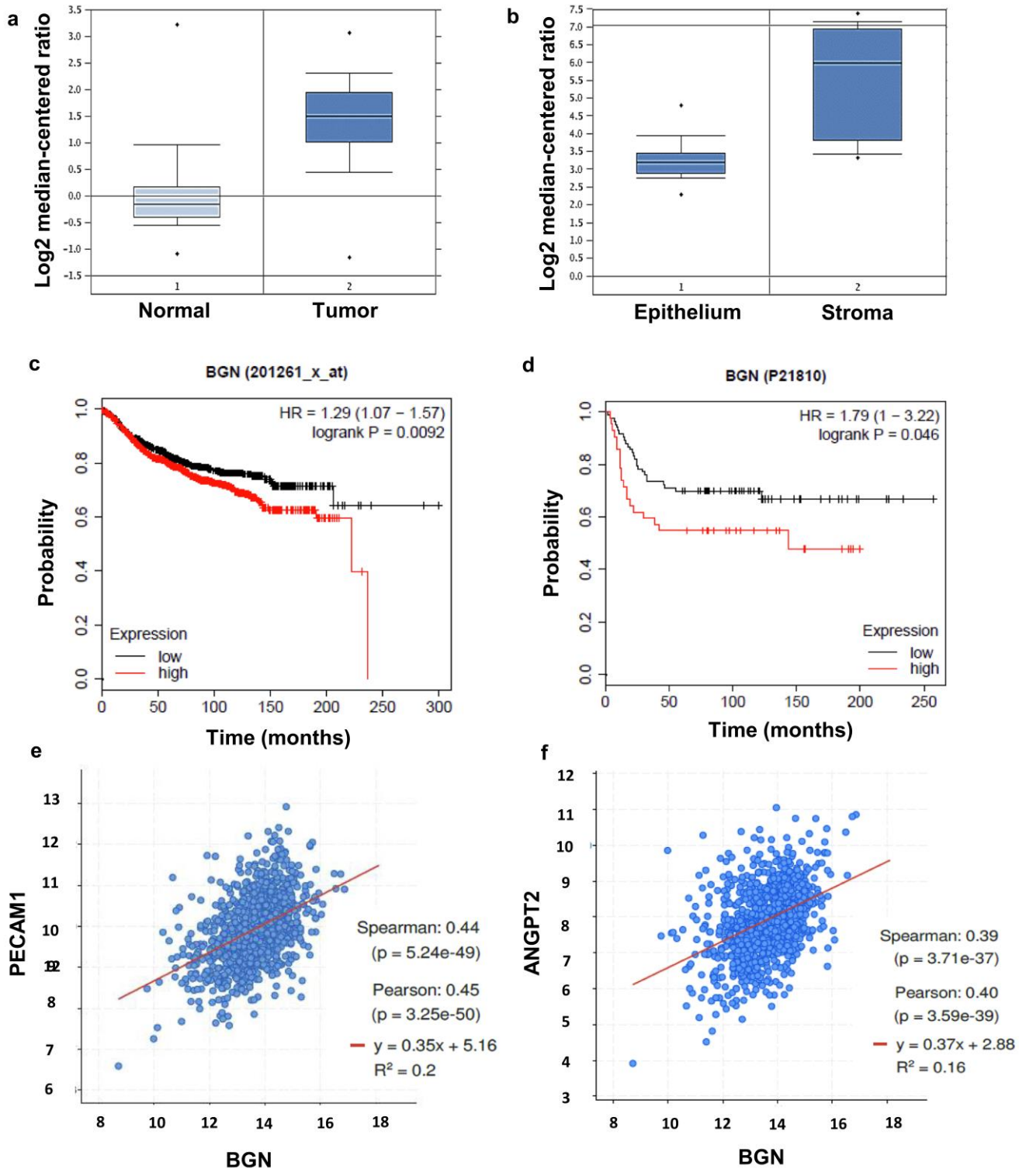

Figure 1. Biglycan is highly expressed in tumor stroma, associated with angiogenesis gene expression and prognosis of human breast cancer patients.

a) Comparison of biglycan mRNA expression was analyzed in normal mammary glands (n = 61) and

breast cancer tissue (n = 389) using Oncomine. b) Comparison of biglycan mRNA expression was analyzed in 14 patient-matched tumor epithelium and tumor-associated stroma specimens using Oncomine. c) Kaplan-Meier analysis was used to assess breast cancer patients with high or low biglycan mRNA expression in distant metastasis-free survival (DMFS) using a Kaplan-Meier plotter tool. d) Kaplan-Meier analysis was used to assess breast cancer patients with high or low biglycan protein expression in DMFS using a Kaplan-Meier plotter tool. e) Correlation between BGN and PECAM1 expression using cBioPortal database. f) Correlation between BGN and ANGPT2 expression using cBioPortal database.

Lung metastasis was decreased in *Bgn* KO mice

To investigate how stromal biglycan affects breast cancer growth and progression, we selected E0771 breast cancer cells derived from C57BL/6 mice and confirmed that E0771 cells had low expression of biglycan (Fig. 2a). Different concentrations of recombinant biglycan also had no significant effect on proliferation of E0771 cells *in vitro* (Fig. 2b). Next, we orthotopically implanted murine E0771 breast carcinoma cells into the mammary fat pads of WT and *Bgn* KO female mice. We confirmed the genotype of the mice used in this study by PCR yielding bands of 212 bp for WT and 310 bp for targeted biglycan allele (Fig. 2c). *Bgn* deficiency resulted in no significant toxic effects in mice, except for a reduced growth rate and decreased bone mass (Corsi et al., 2002; Xu et al., 1998). No significant differences were seen in primary E0771 tumor growth and tumor weight between the WT and *Bgn* KO (Fig. 2d, e). However, *Bgn* KO mice showed reduced lung metastasis confirmed by H&E staining analysis and IVIS (Fig. 2f-i). Furthermore, sentinel lymph node metastasis reduced in *Bgn* KO mice with minimally difference (Fig. 2 h). As E0771 cells had low expression of biglycan *in vitro*, these results suggested that stroma biglycan is involved in lung metastasis but not in tumor growth, consistent with our previous report showing induction of metastasis by biglycan-secreting TECs (Maishi et al., 2016).

a

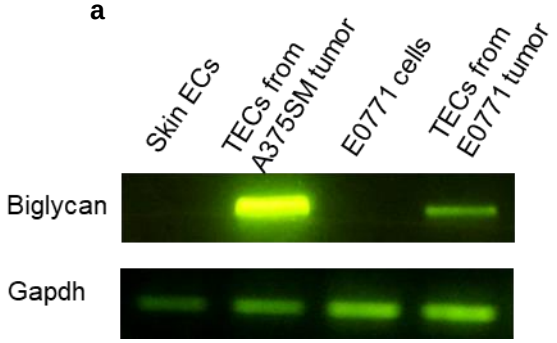

b

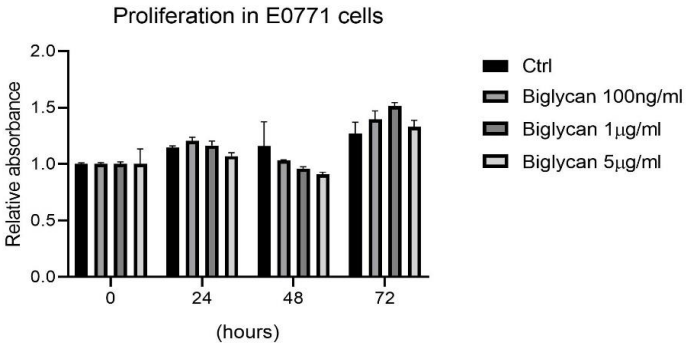

c

WT= 212 bp KO= 310 bp

d

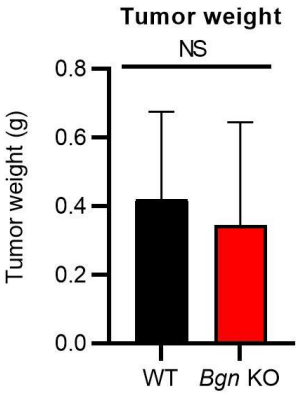

e

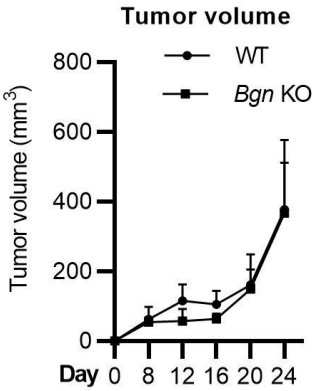

f

Lungs:

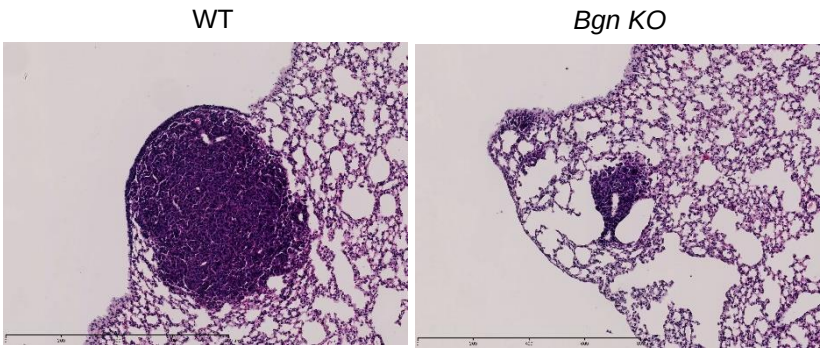

g

	Incidence of metastasis
WT mice	**3/5**
***Bgn* KO mice**	**1/5**

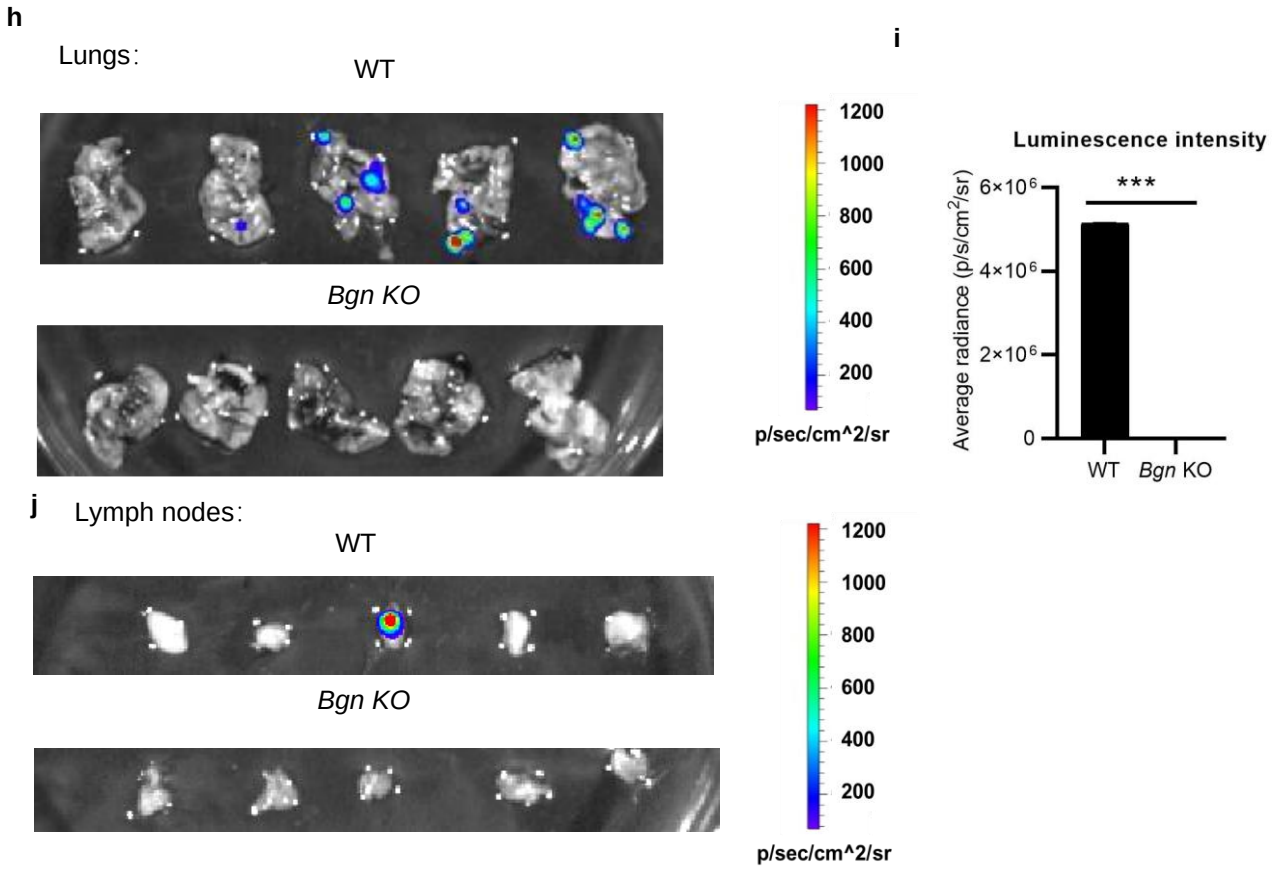

Figure 2. Stromal biglycan inhibition suppresses lung metastasis.

a) Biglycan expression was determined by RT-PCR. Skin ECs and TECs derived from A375SM tumors were negative control and positive control of biglycan expression, as previously reported. b) The proliferation of E0771 cells treated with recombinant biglycan (100 ng/ml, 1 μg/ml and 5 μg/ml) was performed using an MTS assay after 24 h, 48 h, and 92 h. $p > 0.05$. c) Genotyping of *Bgn* KO mice by PCR. d) Growth curves of E0771 tumor growth in WT and *Bgn* KO mice measured every four days. e) Comparison of E0771 tumor weight at day 24 after inoculation. f) H&E staining analysis of metastatic lungs in E0771 tumor of WT versus *Bgn* KO mice. g) The incidence of lung metastasis from E0771 tumors. h, i) Representative IVIS images and quantitative analysis of metastatic lungs in E0771 tumors of WT versus *Bgn* KO mice. j) Representative IVIS images of metastatic lymph nodes in E0771 tumors of WT versus *Bgn* KO mice.

Biglycan was expressed in tumor blood vessels.

We then investigated biglycan expression in the mouse E0771 tumor model. As expected, *Bgn* KO mice showed markedly reduced levels of biglycan mRNA expression in tumor tissues compared to WT mice (Fig. 3a). As biglycan is secreted in a soluble form during inflammation (Poluzzi et al., 2019), we analyzed biglycan concentrations in the plasma of mice. Biglycan concentration was highest in tumor-bearing WT mice compared to non-tumor WT mice and tumor-bearing *Bgn* KO mice (Fig. 3b). Biglycan and CD31 were co-localized by immunofluorescence staining using CD31 and biglycan antibodies (Fig. 3c). Furthermore, to confirm the expression of biglycan in TECs, we isolated TECs from E0771 tumors in WT mice and characterized them as described previously (Yamamoto et al., 2012). The percentage of CD31(+) CD45(-) cells in E0771 tumors was 1.4% consistent with previous report (Fig. 3d). After MACS, the percentage of CD31(+) increased to 36.3% (Fig. 3e). Then we performed FACS sorting using anti-CD31 and anti-CD45 antibodies to purify CD31(+) cells (Fig. 3f). TECs were shown to be negative for the monocyte markers CD11b and CD45, and positive for EC markers CD31, CD144, and CD105 by RT-PCR (Fig. 3g). TECs were positive for EC markers CD31, CD105, and lectin, and negative for the hematopoietic marker CD45 by flow cytometry analysis (Fig.3 h). Isolated cells were also positive for CD31 expression by immunocytochemistry using MS1 cells as the positive control of CD31 expression (Fig. 3i). These results indicate that isolated cells were highly purified ECs. We analyzed *Bgn* mRNA expression in TECs isolated from E0771 tumors (E0771-TECs), isolated CD31-negative cells including tumor cells, fibroblasts, and immune cells, and commercially available dermal ECs from normal mice (NECs) by real-time PCR. *Bgn* mRNA expression was significantly higher in E0771-TECs compared to CD31-negative cells and dermal ECs (Fig. 3j), indicating that TECs were a source of biglycan in E0771 tumor

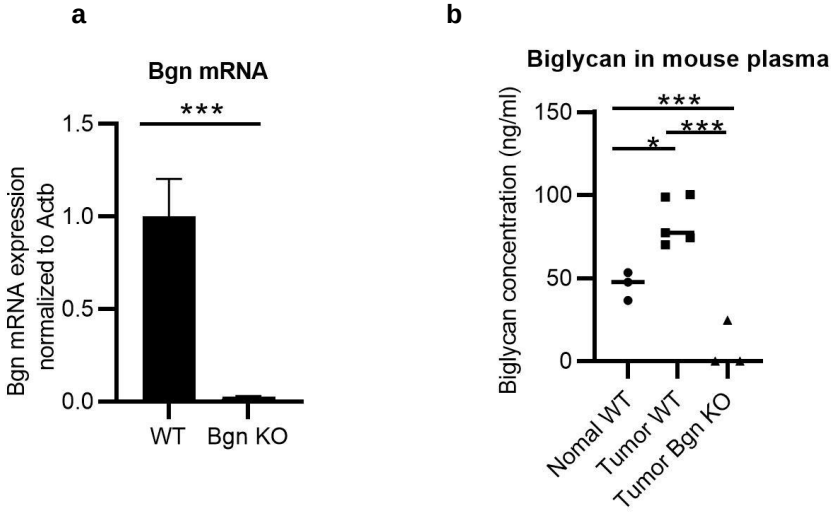

c

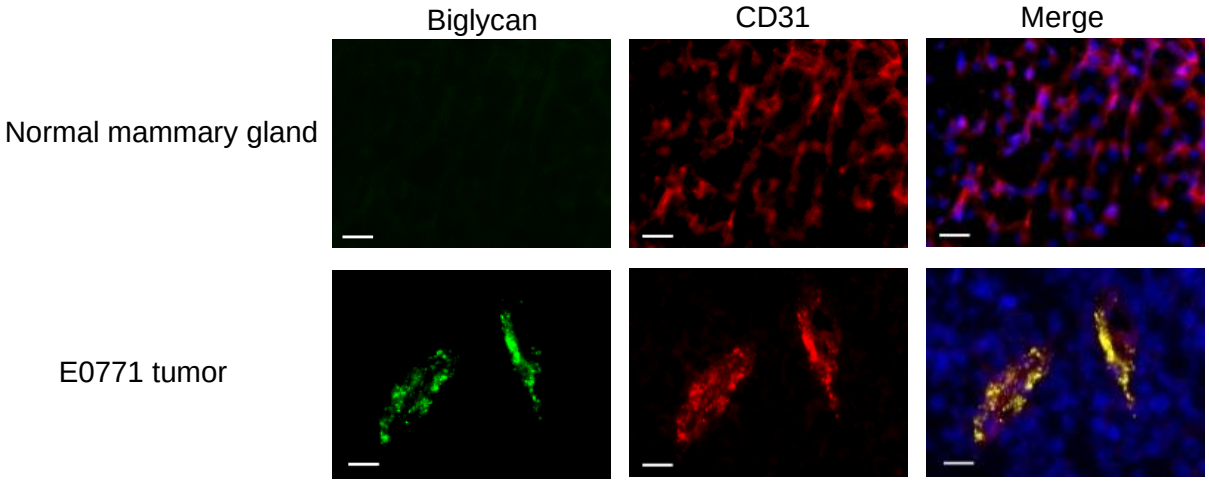

d

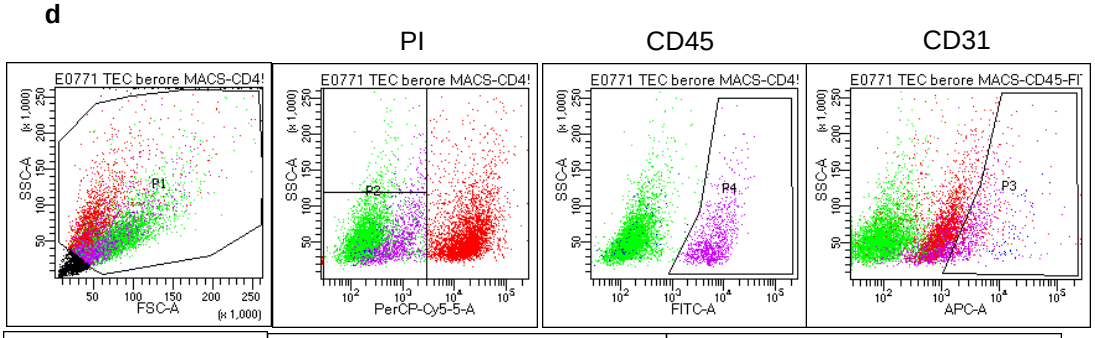

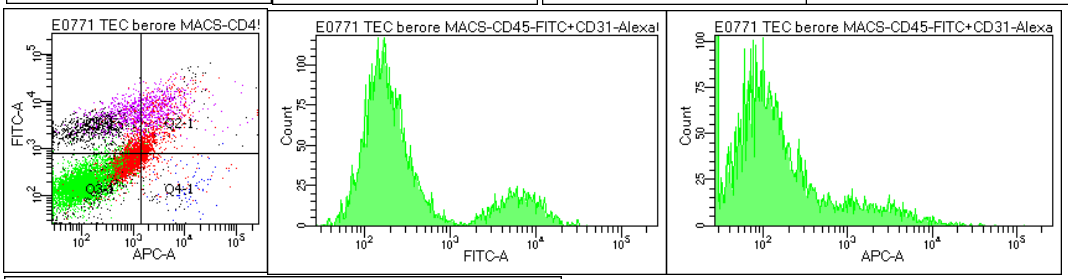

Tube: CD45-FITC+CD31-Alexa647 + PI

Population	#Events	%Parent	%Total
All Events	10,000	####	100.0
P1	8,171	81.7	81.7
P2	4,717	57.7	47.2
P3	432	9.2	4.3
P4	873	18.5	8.7
Q1-1	485	10.3	4.9
Q2-1	460	9.8	4.6
Q3-1	3,706	78.6	37.1
Q4-1	66	1.4	0.7

e

PI CD45 CD31

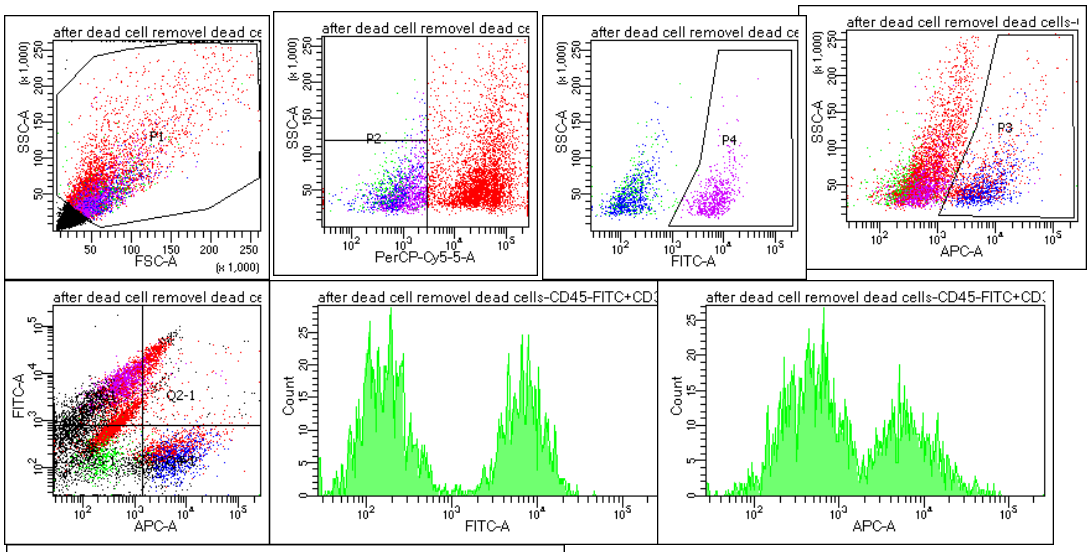

Tube: CD45-FITC+CD31-Alexa647 + PI

Population	#Events	%Parent	%Total
All Events	10,000	####	100.0
P1	5,431	54.3	54.3
P2	1,533	28.2	15.3
P3	563	36.7	5.6
P4	645	42.1	6.4
Q1-1	609	39.7	6.1
Q2-1	50	3.3	0.5
Q3-1	317	[illegible]	3.2
Q4-1	557	36.3	5.6

f

PI Doublet exclusion

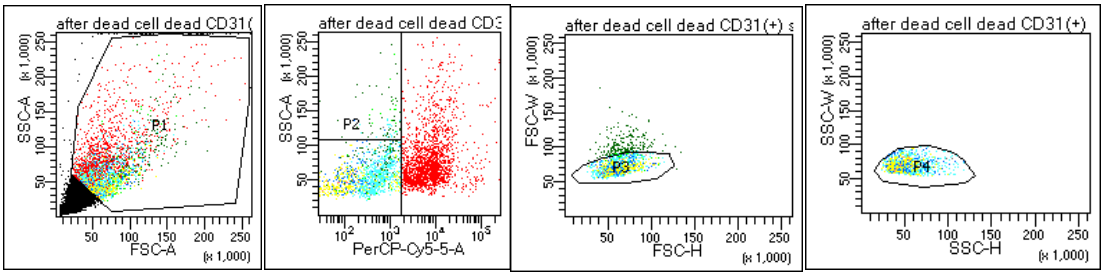

CD45 CD31

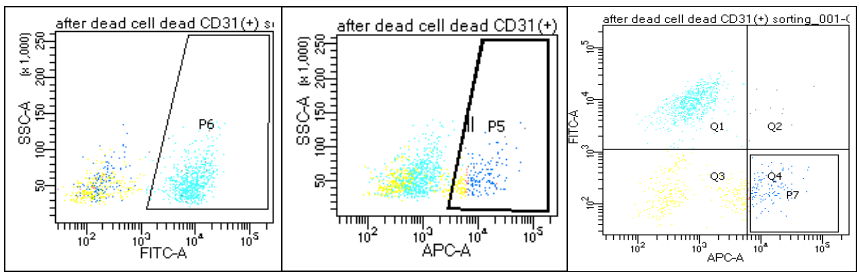

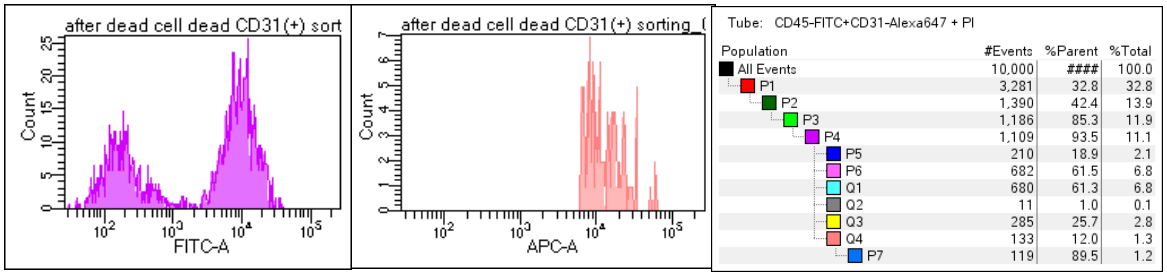
after dead cell dead CD31(+) sort
Count
FITC-A
after dead cell dead CD31(+) sorting_(
Count
APC-A
Tube: CD45-FITC+CD31-Alexa647 + PI
Population #Events %Parent %Total
All Events 10,000 #### 100.0
P1 3,281 32.8 32.8
P2 1,390 42.4 13.9
P3 1,186 85.3 11.9
P4 1,109 93.5 11.1
P5 210 18.9 2.1
P6 682 61.5 6.8
Q1 680 61.3 6.8
Q2 11 1.0 0.1
Q3 285 25.7 2.8
Q4 133 12.0 1.3
P7 119 89.5 1.2

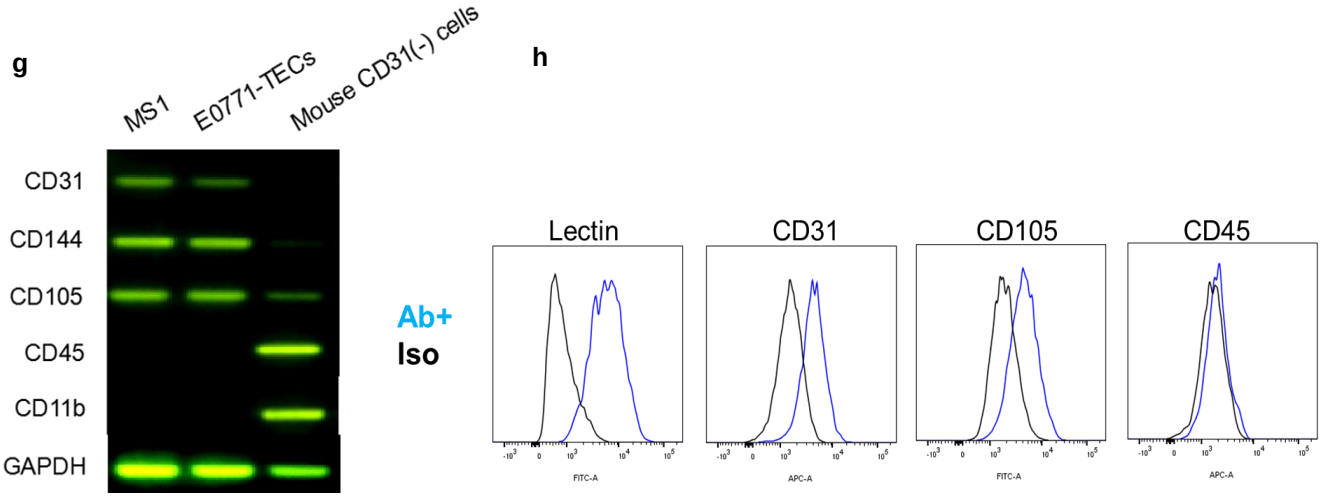
g
MS1
E0771-TECs
Mouse CD31(-) cells
CD31
CD144
CD105
CD45
CD11b
GAPDH
Ab+
Iso
h
Lectin
CD31
CD105
CD45
FITC-A
APC-A
FITC-A
APC-A

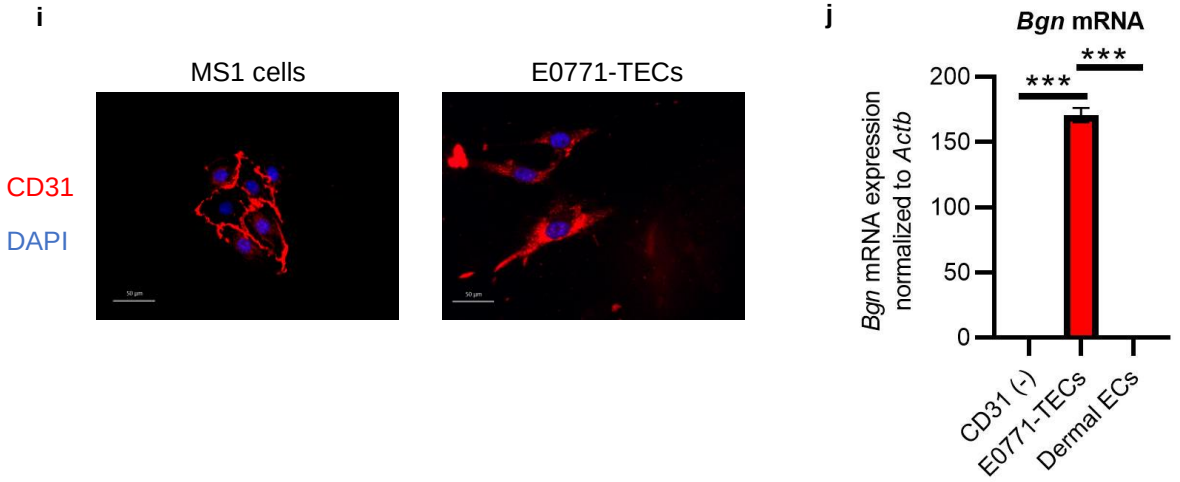
i
MS1 cells
E0771-TECs
CD31
DAPI
j
Bgn mRNA
Bgn mRNA expression normalized to Actb
200
150
100
50
0
***
***
CD31 (-)
E0771-TECs
Dermal ECs

Figure 3. Biglycan was expressed in tumor blood vessels and isolated TECs.

a) *Bgn* mRNA expression in E0771 tumor tissues of WT and *Bgn* KO mic analyzed by quantitative real-time RT-PCR. b) Biglycan concentration in mouse plasma from non-tumor WT mice, E0771 tumor-bearing WT mice, and E0771 tumor-bearing *Bgn* KO mice detected by ELISA. c) Immunofluorescent images of biglycan (green) expression in CD31+ blood vessels (red) in E0771 tumors grown in WT mice. DAPI, blue. Scale bar = 20μm. d) FACS analysis of TECs in E0771 tumors. e) After MACS, FACS analysis of the sorted CD31 (+) cells. f) FACS gating and sorting of CD31(+) cells after MACS. g) E0771-TECs were positive for CD31, CD105, and CD144 by RT–PCR. Mouse tumor stromal CD31- cells were also analyzed. TECs were negative for the monocyte marker CD11b and haematopoietic marker CD45. h) The binding of lectin BS1-B4 and expression of CD31 and CD105 (blue line), and negative expression of CD45 indicated the high purity of isolated TECs. The isotype control is shown as a black line. i) Representative images of CD31 staining in MS1 cells and E0771-TECs. j) *Bgn* mRNA expression in FACS isolated CD31- cells, CD45- CD31+ cells (E0771-TECs), and dermal ECs from naïve mice by quantitative real-time RT-PCR.

Tumor angiogenesis was impaired and tumor blood vessels were normalized in *Bgn* KO mice

To determine the contribution of biglycan to angiogenesis, we first analyzed CD31+ blood vessel density in normal mammary glands from WT and *Bgn* KO mice. No significant changes were observed in morphology and density of normal mammary gland blood vessels in *Bgn* KO and WT mice which means that biglycan has no effect on angiogenesis in normal condition (Fig. 4a, b). Next, we evaluated the microvessel density in E0771 tumors from WT and *Bgn* KO mice. The CD31+ tumor blood vessels were significantly decreased in *Bgn* KO mice as compared to the WT (Fig. 4c, d). Additionally, pericytes surround the vascular endothelium and are often used as an indicator of blood vessel function and integrity and can be detected via α-SMA expression. The percentage of α-SMA+ pericyte-covered blood vessels was significantly higher in *Bgn* KO mice, which indicated that more mature blood vessels existed in tumors from *Bgn* KO mice compared to WT mice (Fig. 4e, f). These data suggested that tumor blood vessels in *Bgn* KO mice are structurally normalized.

Since normalization of tumor blood vessels can also enhance the functions of blood vessels by enhancing blood flow within vessels, we further assessed the vascular function in E0771 tumors in WT

and *Bgn* KO mice. First, by intravenous lectin injection, we identified an increase in lectin-positive (functional) vessels in E0771 tumors of *Bgn* KO mice as compared to those in the WT mice, implying that intratumoral blood perfusion was enhanced in *Bgn* KO mice (Fig. 4g, dh). Tumor vascular normalization is also known to elicit enhanced tumor oxygenation (Stylianopoulos et al., 2018); thus, we analyzed tumor hypoxia by staining tumor tissues with a glucose transporter 1 (Glut1) antibody (Fig. 4i, j). Glut1+ area was decreased in tumors of *Bgn* KO mice compared to WT mice. As hypoxic response is mainly ascribed to hypoxia-inducible factor-1 (HIF-1) α which is involved in the induction of Glut1 expression (Hayashi et al., 2004), we checked whether biglycan affects HIF1-α and Glut1 expression in tumor cells. We found that Hif1a and Slc2a1 expression elevation in E0771 cells by stimulation with recombinant biglycan (Fig.4 k, l), which indicated that biglycan might mediate HIF1-α and Glut1 expression in tumor cells. Together, these data suggested that alleviating tumor hypoxia by biglycan knockout might be due to enhancement of vascular normalization and mediation of HIF1-α and Glut1 expression in tumor cells.

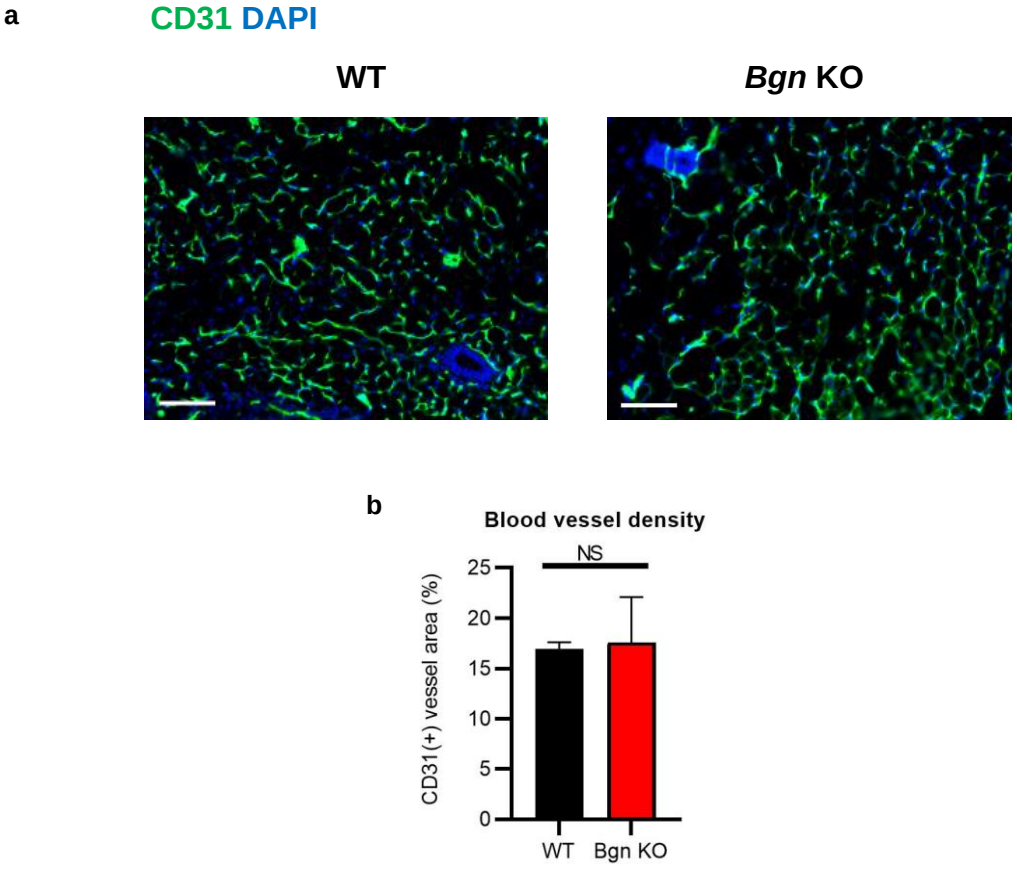

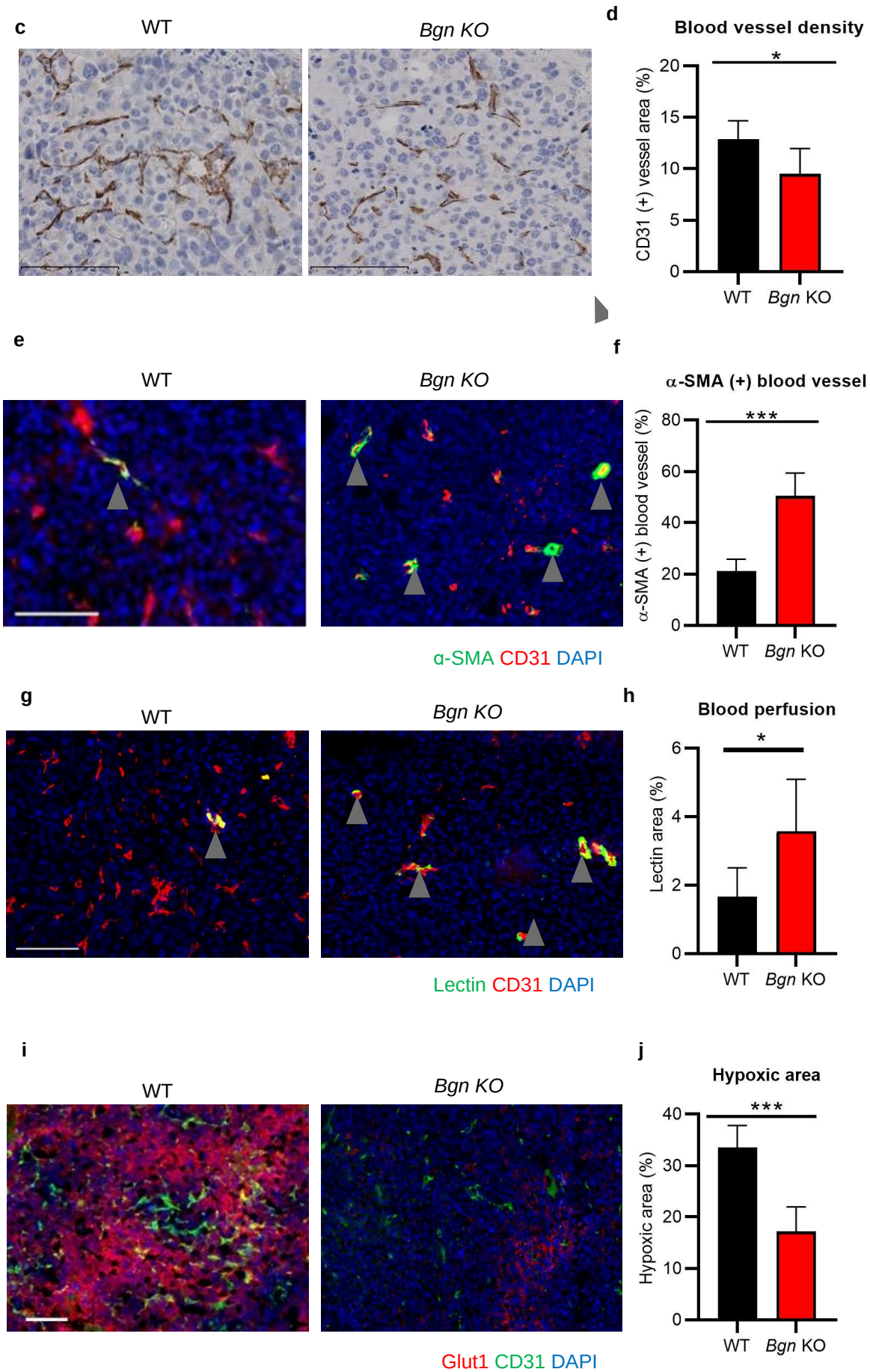
c
WT
Bgn KO
d
Blood vessel density
CD31 (+) vessel area (%)
20
15
10
5
0
*
WT
Bgn KO
e
WT
Bgn KO
α-SMA CD31 DAPI
f
α-SMA (+) blood vessel
α-SMA (+) blood vessel (%)
80
60
40
20
0
***
WT
Bgn KO
g
WT
Bgn KO
Lectin CD31 DAPI
h
Blood perfusion
Lectin area (%)
6
4
2
0
*
WT
Bgn KO
i
WT
Bgn KO
Glut1 CD31 DAPI
j
Hypoxic area
Hypoxic area (%)
40
30
20
10
0
***
WT
Bgn KO

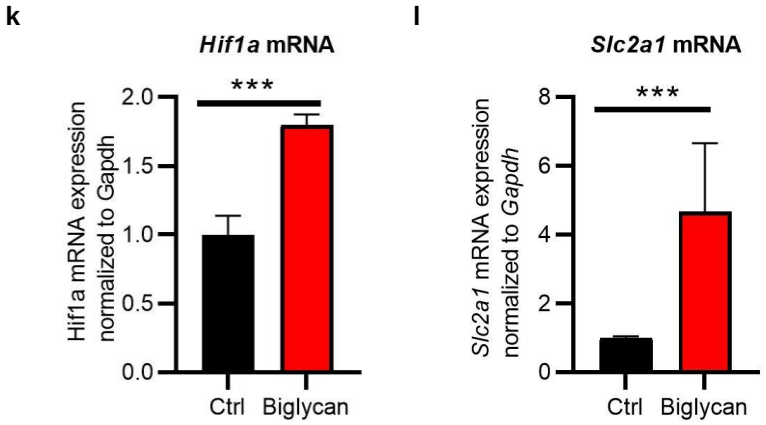

Figure 4. Stromal biglycan inhibition normalized tumor vasculature in breast cancer.

a) Representative images of CD31+ blood vessels in normal mammary glands from WT and *Bgn* KO mice. b) Quantification of blood vessel density. n=3 mice per group. c) Representative images of CD31+ blood vessels in E0771 tumors from WT and *Bgn* KO mice. Scale bar = 100μm. d) Quantification of blood vessel density. e) Representative images of CD31 immunostaining (red), α-SMA (green), and DAPI nuclear staining (blue) in E0771 tumors from WT and *Bgn* KO mice. Scale bar = 100μm. f) Quantification of α-SMA+ CD31+ tumor blood vessels. The rate of microvessel pericyte coverage was analyzed by counting the vessels that stained positive for both CD31 and α-SMA (white arrowheads) among CD31-positive vessels. g) Representative images of CD31 immunostaining (red), FITC-lectin (green) and DAPI (blue) in E0771 tumors from WT and *Bgn* KO mice. Scale bar = 100μm. h) Quantification of lectin+ blood vessels. The rate of lectin+ blood vessels was analyzed by counting the vessels that stained positive for both CD31 and lectin (white arrowheads) among CD31-positive vessels. i) Representative images of CD31 immunostaining (green), Glut1 (red), and DAPI (blue) in E0771 tumors from WT and *Bgn* KO mice. Scale bar = 100μm. j) Quantification of Glut1+ area. k) *Hif1a* mRNA expression in E0771 cells treated with

recombinant biglycan (5μg/ml) by quantitative RT-PCR. l) *Slc2a1* mRNA expression in E0771 cells treated with recombinant biglycan (5μg/ml) by quantitative RT-PCR.

Angpt2 expression was decreased in E0771 tumors from *Bgn* KO mice

Vascular normalization is regulated by several molecules, such as ANG-TIE, PDGFB, and NG2 (Carmeliet and Jain, 2011b). BGN was positively correlated with ANGPT2 expression in human breast cancers (Fig. 1f). We next confirmed that *Angpt2* mRNA expression was decreased in tumor tissues from *Bgn* KO mice (Fig. 5a). To determine whether biglycan has any direct effect on *Angpt2* expression, we stimulated MS1 cells (immortalized normal ECs) with recombinant biglycan after confirming the expression of the biglycan receptors, Toll-like receptors (TLRs) 2 and 4 in the MS1 cells (Fig. 5b). There was no significant difference in *Angpt2* expression between biglycan-treated and non-treated cells (Fig. 5c). Furthermore, biglycan knockdown in E0771-TECs (Fig. 5d) did not alter *Angpt2* mRNA expression in the cells. (Fig. 5e). Therefore, we speculated that biglycan may not regulate *Angpt2* expression in ECs directly via its receptors, but rather by other indirect mechanisms. We further analyzed the molecular relationship between biglycan and ANGPT2 by Ingenuity Pathway Analysis (IPA, Tomy Digital Biology). Signature genes which are not only mediated by biglycan during inflammation but also involved in pro-angiogenetic signaling pathways such as Il1b, Ccl2, Ccl5 and Tnf were added in the flow between biglycan and Angpt2. We found that only Tnf was matched to mediate this interaction between biglycan and Angpt2 (Fig. 5f). As TNF-α is not directly angiogenetic, we hypothesized that Angpt2 might be controlled by biglycan/TNF-α signaling on the regulation of destabilizing tumor blood vessels.

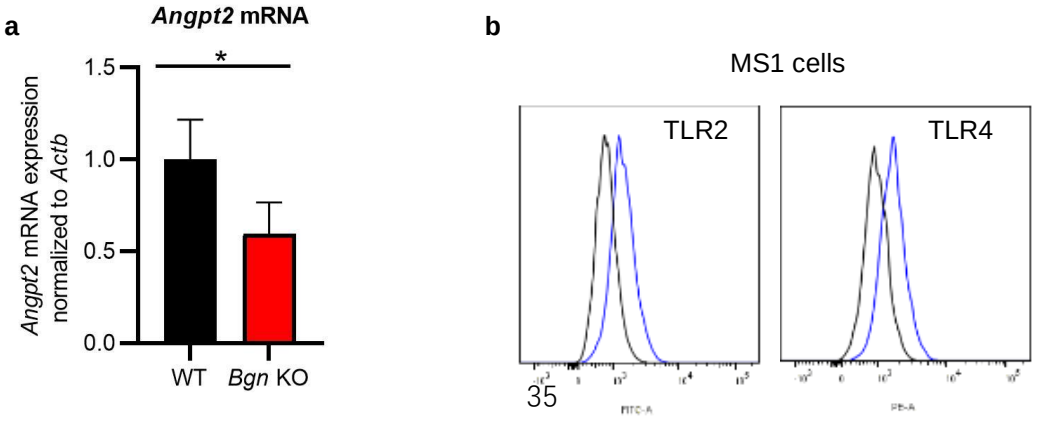

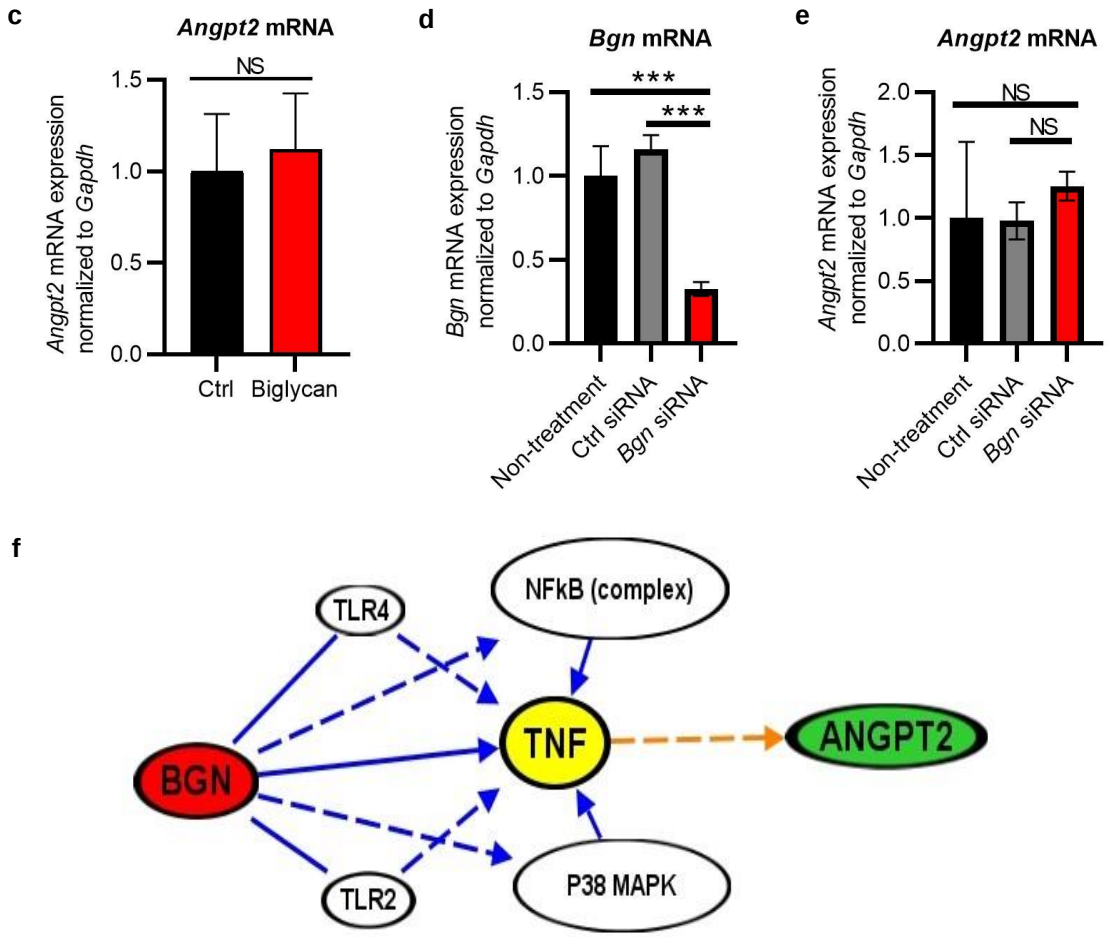

Figure 5. Angpt2 expression was decreased in E0771 tumors from *Bgn* KO mice.

a) *Angpt2* mRNA expression in E0771 tumor tissues of WT and *Bgn* KO mice by quantitative real-time PCR. b) TLR2 and TLR4 expression in MS1 cells analyzed by FACS analysis. Blue: antibody. Black: isotype. c) *Angpt2* mRNA expression in MS1 cells treated with recombinant biglycan (5 g/ml) by quantitative real-time RT-PCR. d) *Bgn* mRNA expression in E0771-TECs transfected with *Bgn* siRNA by quantitative real-time PCR. e) *Angpt2* mRNA expression in E0771-TECs transfected with *Bgn* siRNA by quantitative real-time PCR. f) Flow chart of biglycan, TNF-α, and *Angpt2* signaling by IPA analysis.

TNF-α-enhanced Angpt2 expression is controlled by biglycan through activation of NF-

κB and ERK via TLR2/4

We compared *Tnf* mRNA expression and TNF-α secretion in E0771 tumor bearing WT and *Bgn* KO mice. *Bgn* KO mice showed significantly reduced *Tnf* mRNA expression in E0771 breast cancer tissues and TNF-α secretion in plasma from tumor-bearing mice (Fig.6a, b). As soluble biglycan can bind to TLRs 2 and 4 on macrophages and activate mitogen-activated protein kinase (MAPK) p38, extracellular signal-regulated kinase (ERK), and nuclear factor-κB (NF-κB) signaling pathways (Schaefer et al., 2005), we confirmed that E0771 cells expressed TLR2 and TLR4 by flow cytometry analysis (Fig. 6c). We proceeded to investigate the paracrine effects of biglycan on TNF-α expression in E0771 cells (Fig. 6d) and RAW macrophages (Fig.6e) stimulated with recombinant biglycan. *Tnf* mRNA expression was significantly increased in biglycan-stimulated cells as compared to non-treated control cells. Blockage of the Bgn-TLR2 or -TLR4 interaction in E0771 cells by neutralizing antibodies significantly decreased *Tnf* mRNA expression in E0771 cells stimulated with recombinant biglycan (Fig. 6f, g), suggesting that biglycan regulates TNF-α expression in tumor cells through binding to TLR2 and TLR4. To elucidate the downstream mediators of *Tnf* induction, E0771 cells were first pretreated with the NF-κB inhibitor BAY11-7082 or the ERK inhibitor U1026, and then stimulated with recombinant biglycan. NF-κB or ERK blockade decreased *Tnf* mRNA expression (Fig. 6h, i), indicating that biglycan may regulate TNF-α expression through NF-κB and ERK signaling pathways.

Furthermore, we analyzed the effect of biglycan on TNF-α expression in ECs. The *Tnf* mRNA expression level in MS1 cells was not changed significantly after stimulation with recombinant biglycan (Fig.6 j). In addition, *Tnf* expression showed no difference between biglycan knockdown E0771-TECs and controls (Fig.6 k), implying that biglycan has no autocrine effect on TNF-α expression. In order to confirm that TNF-α can indeed induce *Angpt2* expression in ECs, we confirmed the presence of TNFR1 and TNFR2 expression in ECs (Fig.6 l), and stimulated MS1 cells with TNF-α. This led to increased levels of *Angpt2* mRNA in MS1 cells (Fig.6 m), consistent with previous reports. These data indicated that biglycan may regulate *Angpt2* expression via enhanced levels of TNF-α indirectly in a paracrine manner (Fig. 7).

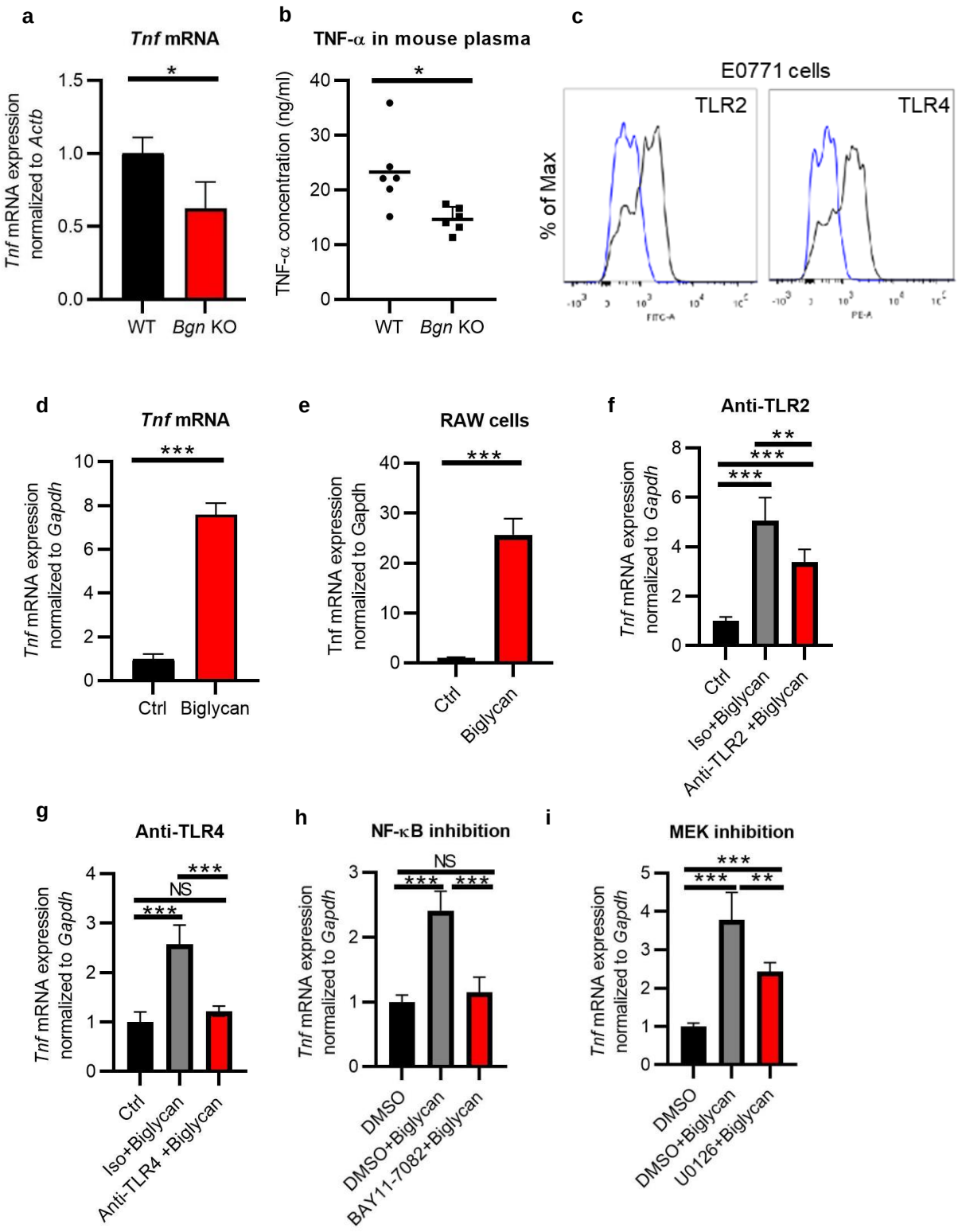
a
Tnf mRNA
Tnf mRNA expression normalized to Actb
1.5
1.0
0.5
0.0
*
WT
Bgn KO
b
TNF-α in mouse plasma
TNF-α concentration (ng/ml)
40
30
20
10
0
*
WT
Bgn KO
c
E0771 cells
TLR2
TLR4
% of Max
FITC-A
PE-A
d
Tnf mRNA
Tnf mRNA expression normalized to Gapdh
10
8
6
4
2
0
***
Ctrl
Biglycan
e
RAW cells
Tnf mRNA expression normalized to Gapdh
40
30
20
10
0
***
Ctrl
Biglycan
f
Anti-TLR2
Tnf mRNA expression normalized to Gapdh
8
6
4
2
0
**
***
***
Ctrl
Iso+Biglycan
Anti-TLR2 +Biglycan
g
Anti-TLR4
Tnf mRNA expression normalized to Gapdh
4
3
2
1
0
***
NS
***
Ctrl
Iso+Biglycan
Anti-TLR4 +Biglycan
h
NF-κB inhibition
Tnf mRNA expression normalized to Gapdh
3
2
1
0
NS
***
***
DMSO
DMSO+Biglycan
BAY11-7082+Biglycan
i
MEK inhibition
Tnf mRNA expression normalized to Gapdh
5
4
3
2
1
0
***
***
**
DMSO
DMSO+Biglycan
U0126+Biglycan

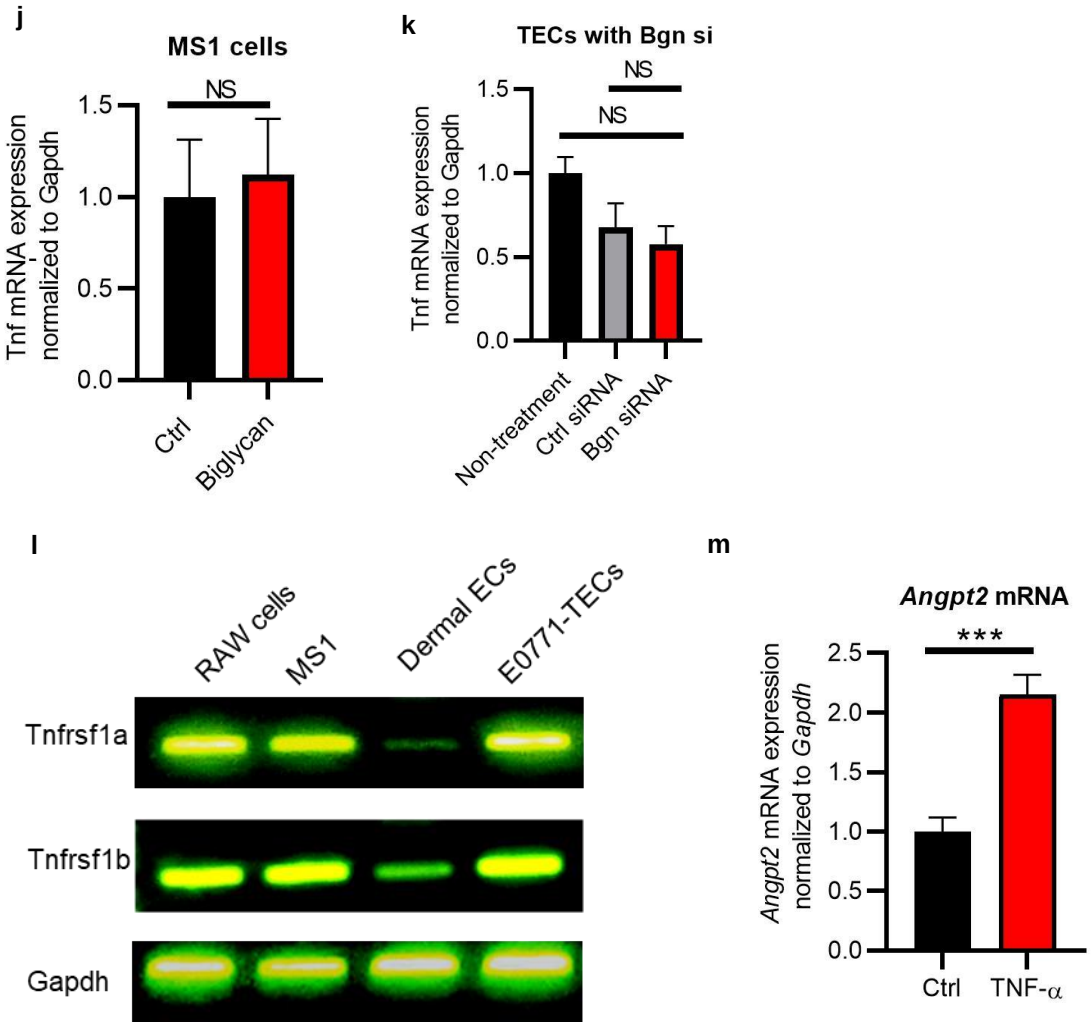

Figure 6. TNF-α-enhanced Angpt2 expression is controlled by biglycan in E0771 tumors.

a) *Tnf* mRNA expression by quantitative RT-PCR in E0771 tumor tissues from WT and *Bgn* KO mice. b) TNF-α secretion in the plasma of E0771 tumor-bearing mice was detected by ELISA. Each dot represents one mouse. c) TLR2 and TLR4 expression in E0771 cells analyzed by flow cytometry. Blue: isotype. Black: antibody. d) *Tnf* mRNA expression in E0771 cells treated with recombinant biglycan (5μg/ml). e) *Tnfa* mRNA expression in RAW cells treated with recombinant biglycan (5 μg/ml) by quantitative RT-PCR. f) After blocking

of TLR2 or (g) TLR4 (l), E0771 cells were stimulated by recombinant biglycan (5μg/ml). *Tnf* mRNA expression was analyzed by quantitative RT-PCR. h,i) After treating with (m) the NF-κB inhibitor (10μM) or (n) the MEK inhibitor (20μM), E0771 cells were stimulated by recombinant biglycan (5μg/ml). *Tnf* mRNA expression was analyzed by quantitative real-time RT-PCR. j) *Tnfa* mRNA expression in MS1 cells treated with recombinant biglycan (5 μg/ml) by quantitative RT-PCR. k) *Tnfa* mRNA expression in E0771-TECs transfected with *Bgn* siRNA by quantitative RT-PCR. l) Expression of TNFR1 (*Tnfrsf1a*) and TNFR2 (*Tnfrsf1b*) in MS1 cells, dermal ECs, and E0771-TECs by RT-PCR. RAW cells were used as a positive control. m *Angpt2* mRNA expression in MS1 cells treated with recombinant TNF-α (10 ng/ml) by quantitative RT-PCR.

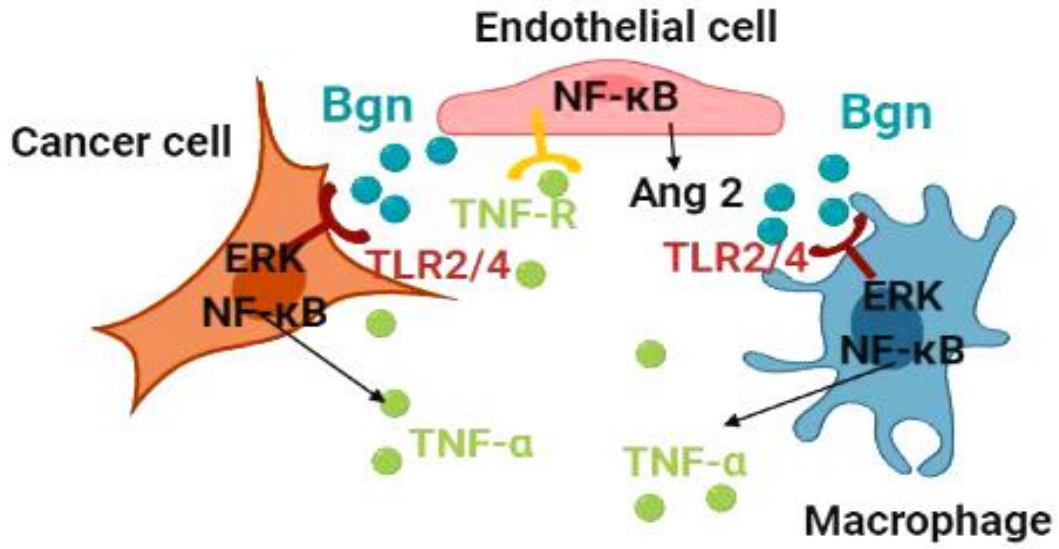

Figure 7. Scheme of biglycan regulating Angpt2. Stromal biglycan enhances TNF-α expression in tumor cells and macrophages, and that TNF-α subsequently upregulates Angpt2 expression in ECs, thus destabilizing tumor blood vessels.

Biglycan inhibition suppresses tumor fibrosis.

Biglycan has been shown to interact with collagen I, and functions in organization of the assembly of the extracellular matrix (Schonherr et al., 1995). Furthermore, as a DAMP, biglycan potentiates renal inflammation and fibrotic renal disorders. (Anders and Schaefer, 2014) Thus, we assessed collagen deposition by picrosirius red staining in E0771 tumors. We found that collagen accumulation was reduced in tumors from *Bgn* KO mice compared to those in WT mice (Fig. 8a, b). *Col1a1* mRNA expression was also decreased in tumor tissues from *Bgn* KO mice (Fig. 8c). Furthermore, biglycan mRNA expression was positively correlated with COL1A1 in human breast cancers (Fig. 8d). These findings indicate that biglycan knockout suppressed tumor fibrosis and biglycan may be involved in tumor fibrosis. As activated cancer-associated fibroblasts (CAFs) in tumor stroma is involved in tumor fibrosis and activated CAFs can be identified by their expression of α-SMA (Sahai et al., 2020), α-SMA+ fibroblast (excluded pericytes) assessment by staining was analyzed in biglycan KO mice. α-SMA+ fibroblasts were significantly decreased in *Bgn* KO mice as compared to the WT mice (Fig. 8 e, f). We also analyzed the effect of biglycan on α-SMA expression in fibroblasts and found that α-SMA mRNA expression was upregulated in NIH3T3 cells by biglycan treatment (Fig. 8g). These results indicate that biglycan may activate fibroblasts via upregulating α-SMA expression.

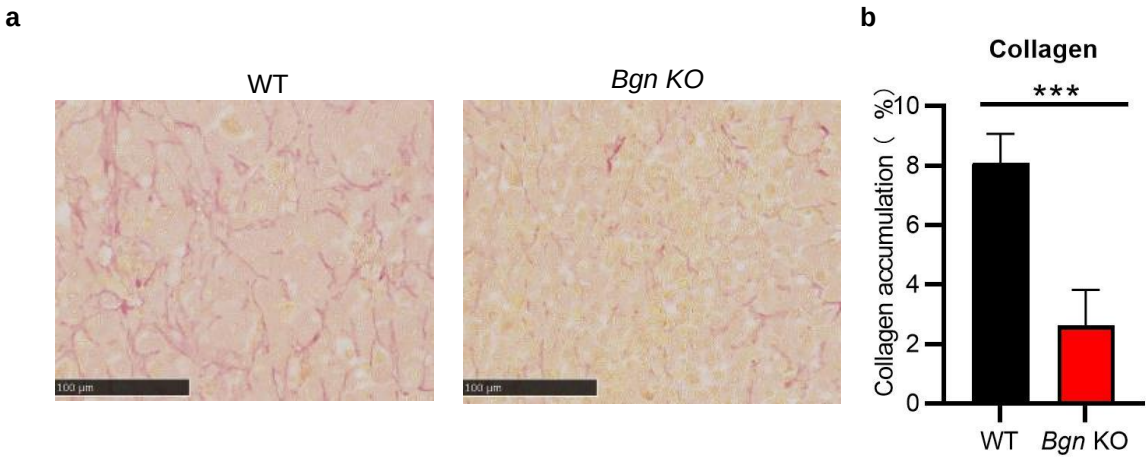

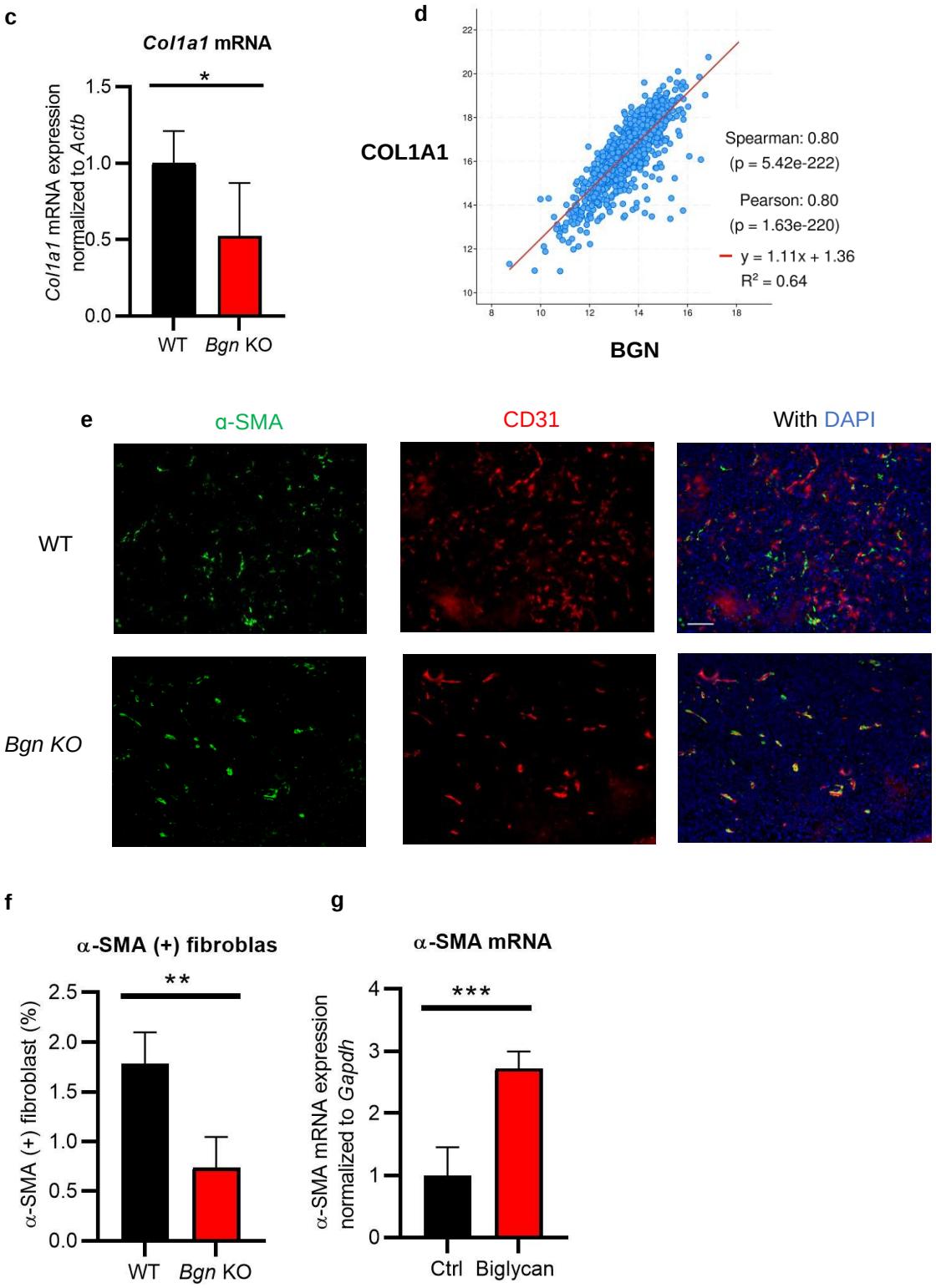
c
Col1a1 mRNA
*
Col1a1 mRNA expression normalized to Actb
1.5
1.0
0.5
0.0
WT
Bgn KO
d
COL1A1
Spearman: 0.80
(p = 5.42e-222)
Pearson: 0.80
(p = 1.63e-220)
y = 1.11x + 1.36
R² = 0.64
BGN
e
α-SMA
CD31
With DAPI
WT
Bgn KO
f
α-SMA (+) fibroblas
**
α-SMA (+) fibroblast (%)
2.5
2.0
1.5
1.0
0.5
0.0
WT
Bgn KO
g
α-SMA mRNA
***
α-SMA mRNA expression normalized to Gapdh
4
3
2
1
0
Ctrl
Biglycan

Figure 8. Biglycan inhibition reduces stromal fibrosis.

a) Representative images of picrosirius red staining for collagen in E0771 tumors from WT and *Bgn* KO mice. Scale bar = 100μm. b) Quantification of collagen accumulation. Data represent means ± SD. n = 5 fields, 5 mice per group. c) *Col1a1* mRNA expression in E0771 tumor tissues of WT and *Bgn* KO mice by quantitative RT-PCR. n = 4 RT-PCR replicates per mouse, 5 mice per group. d) Correlation between BGN and COL1A1 expression using cBioPortal database. e) Representative images of α-SMA (green), CD31 immunostaining (red) and DAPI nuclear staining (blue) in E0771 tumors from WT and *Bgn* KO mice. Scale bar = 100μm.f) Quantification of α-SMA + fibroblasts. The area of α-SMA + fibroblasts was analyzed by excluding α-SMA + pericytes from CD31+ blood vessels. g) α-SMA mRNA expression in NIH3T3 cells treated with recombinant biglycan by quantitative real-time RT-PCR.

Stromal biglycan deficiency increases the recruitment of CD8+ T cells in breast cancer.

The vascular normalization in tumor stroma is reported to increase the accessibility of immune cells to the tumors (Shrimali et al., 2010). Furthermore, a fibrotic tumor microenvironment can suppress the immune response to cancer. (Chen et al., 2019) Therefore, we analyzed the mRNA expression of several immune cell markers (*Cd4*, *Cd8*, *Klrb1c*, *CD27*, and *Adgre1*) within the E0771 tumor tissues from WT and *Bgn* KO mice (Fig. 9a-e). We found that only *Cd8a* mRNA expression was significantly increased in *Bgn* KO mice (Fig. 9e), potentially indicating an accumulation of CD8+ T cells. We confirmed this hypothesis by FACS analysis, which demonstrated that the percentage of CD45+CD8+ T cells was higher in *Bgn* KO mice compared to WT mice (Fig. 9f, g). The infiltration of CD8+ T cells in E0771 tumors was also analyzed by IHC. Quantification of CD8+ T cells by IHC showed a significant increase in *Bgn* KO mice, with lymphocytes distributed throughout the tumor (Fig. 9h, I, j). Together, these data indicate that CD8+ T cell distribution in tumor tissues may be improved by biglycan inhibition.

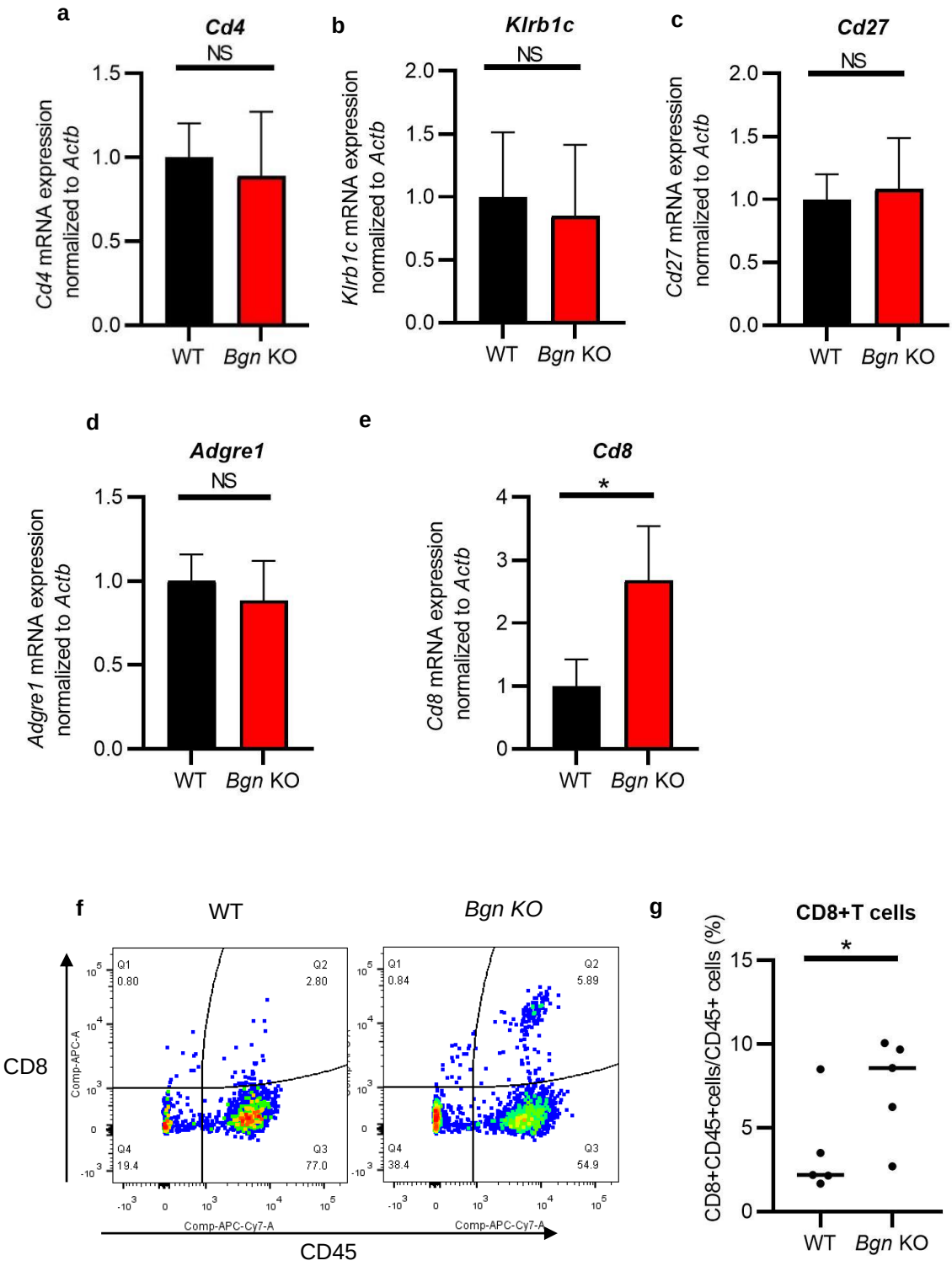
a
Cd4
NS
Cd4 mRNA expression normalized to Actb
1.5
1.0
0.5
0.0
WT
Bgn KO
b
Klrb1c
NS
Klrb1c mRNA expression normalized to Actb
2.0
1.5
1.0
0.5
0.0
WT
Bgn KO
c
Cd27
NS
Cd27 mRNA expression normalized to Actb
2.0
1.5
1.0
0.5
0.0
WT
Bgn KO
d
Adgre1
NS
Adgre1 mRNA expression normalized to Actb
1.5
1.0
0.5
0.0
WT
Bgn KO
e
Cd8
*
Cd8 mRNA expression normalized to Actb
4
3
2
1
0
WT
Bgn KO
f
WT
Bgn KO
CD8
Q1
0.80
Q2
2.80
Q4
19.4
Q3
77.0
Q1
0.84
Q2
5.89
Q4
38.4
Q3
54.9
Comp-APC-A
Comp-APC-Cy7-A
CD45
g
CD8+T cells
*
CD8+CD45+cells/CD45+ cells (%)
15
10
5
0
WT
Bgn KO

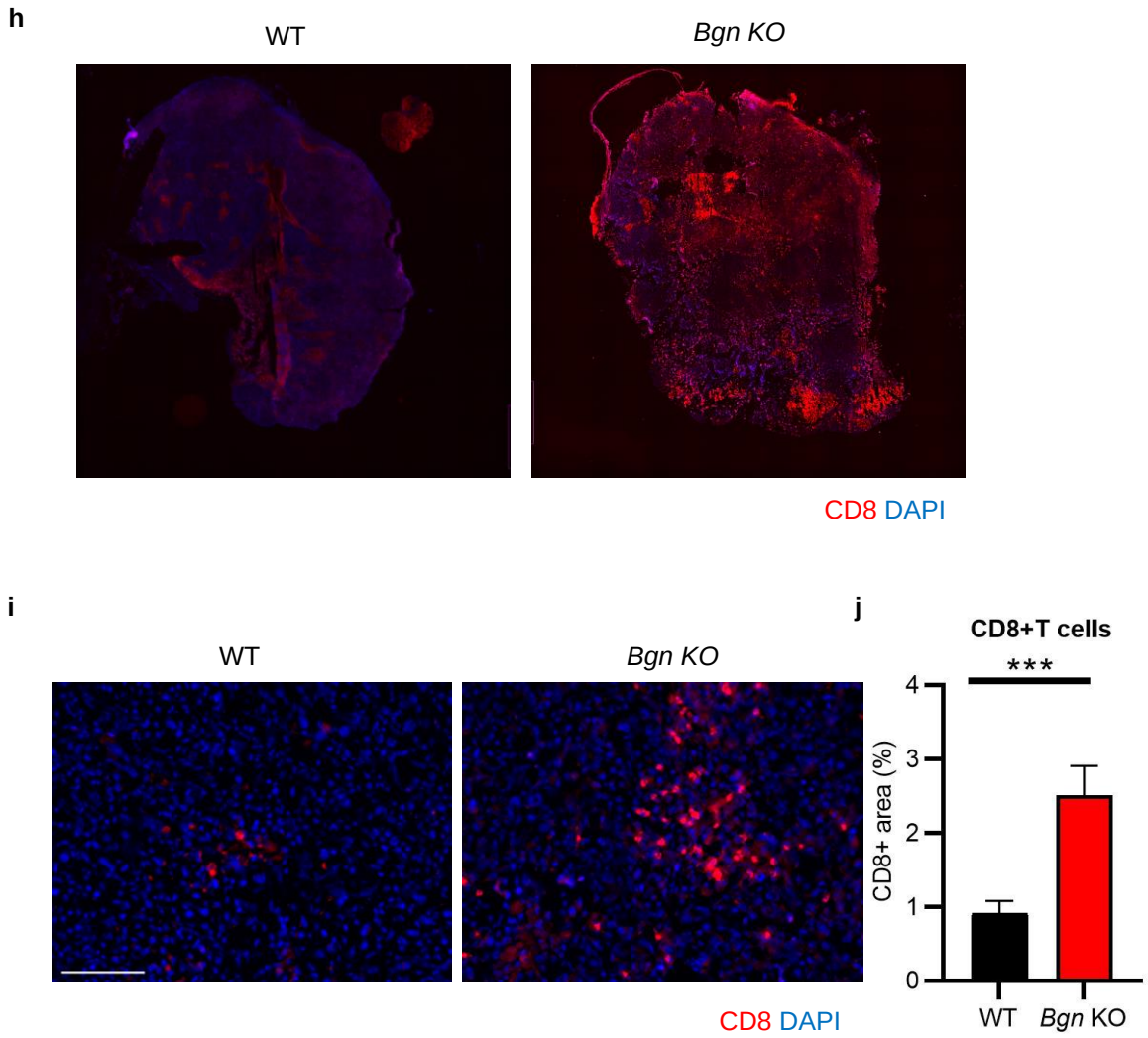

Figure 9. Biglycan inhibition normalizes immune suppressive microenvironment.

a) *Cd4*, b) *Klrb1c*, c) *Cd27*, d) *Adgre1*, and e) *Cd8* mRNA expression by quantitative RT-PCR in E0771 tumor tissues from WT and *Bgn* KO mice. NS, not significant. n = 4 RT-PCR replicates per mouse, 4-5 mice per group. f, g) CD8+CD45+ T cell analysis in E0771 tumors of WT and *Bgn* KO mice by flow cytometry. f) Representative data and g) the percentage of CD8+CD45+ T cells/CD45+ T cells. n = 5 mice per group. h) and i) Representative images of CD8+ T cells in E0771 tumors from WT and *Bgn* KO mice. i) in tumor center, Scale bar = 100μm. j Quantification of CD8+ T cells in tumor center.

Biglycan inactivation enhances drug delivery and the antitumor effect of paclitaxel

Normalization of the tumor microenvironment could potentially improve drug delivery and efficiency of chemotherapy (Chauhan et al., 2013). As tumor blood perfusion was improved and tumor fibrosis was inhibited in *Bgn* KO mice, we measured drug delivery and chemotherapeutic efficacy in E0771 tumors. Doxorubicin delivery was enhanced in *Bgn* KO mice (Fig. 10a, b). Additionally, the chemotherapeutic agent paclitaxel significantly suppressed E0771 tumor growth in *Bgn* KO mice (Fig. 10c). The number of lymph node metastases was decreased in paclitaxel treated *Bgn* KO mice (1/5, 20%) as compared to paclitaxel treated WT mice (2/5, 40%) (Fig. 10d). Paclitaxel treatment also increased the incidence of lung metastasis (2/5, 40%) in WT mice compared to *Bgn* KO mice (0/5) (Fig. 10e). These data suggested that loss of stromal biglycan enhanced chemotherapeutic efficacy in tumors via normalization of breast cancer microenvironment.

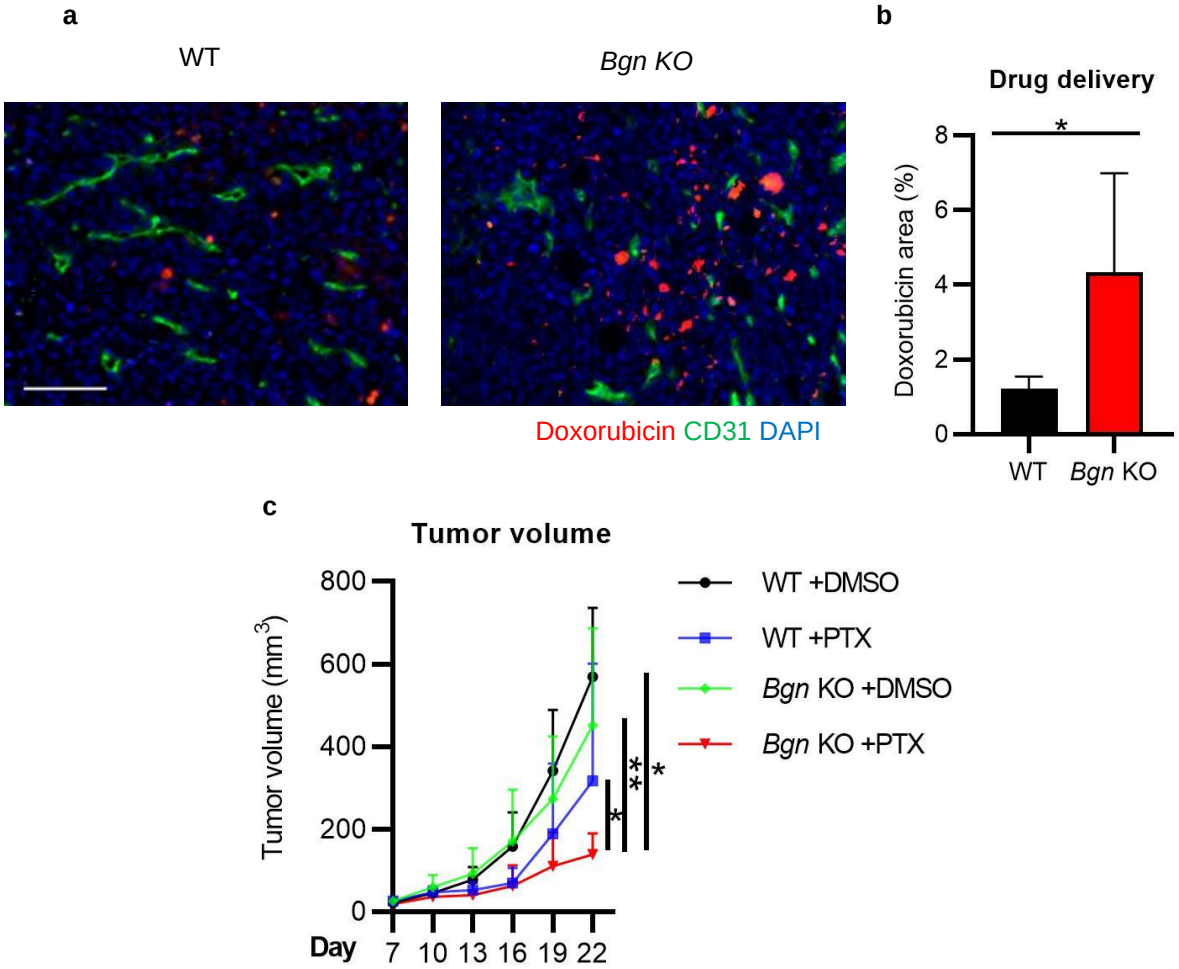

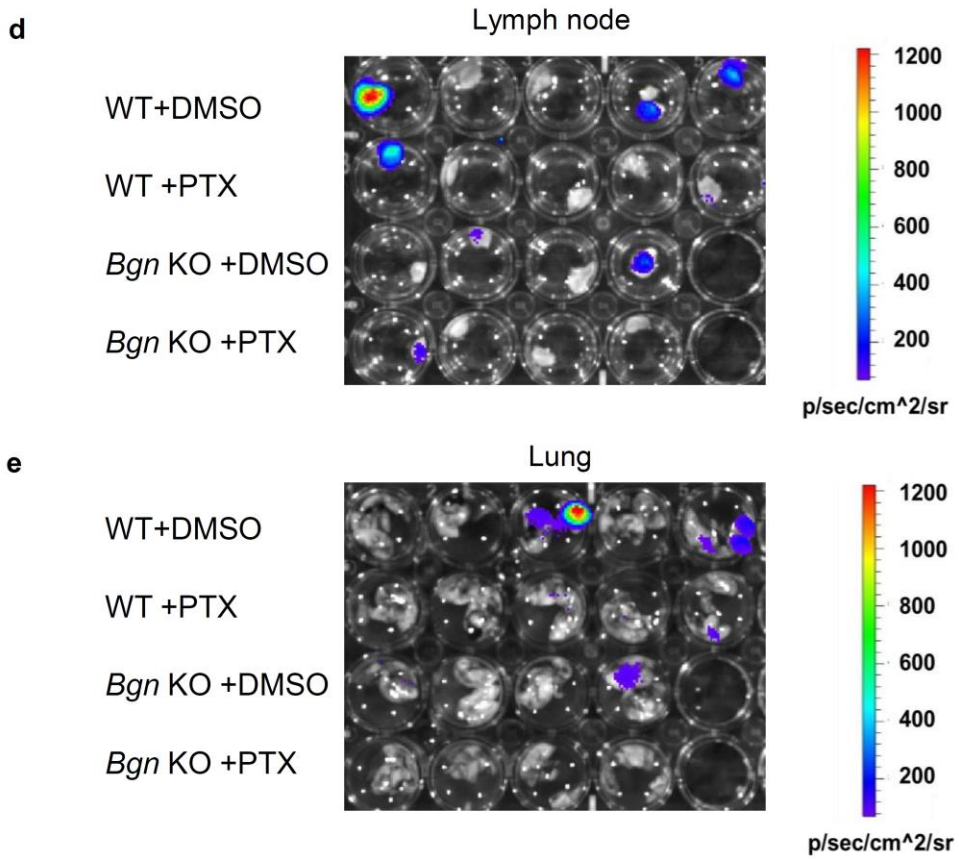

Figure. 10 Biglycan deletion enhances drug delivery and antitumor effect of paclitaxel in breast cancer.

a) Representative images of CD31 immunostaining (green), doxorubicin (red), and DAPI nuclear staining (blue) in E0771 tumors from WT and *Bgn* KO mice. Scale bar = 100μm. b) Quantification of drug delivery. Significance was determined by a two-tailed Student's t-test. n = 5 fields per mouse, 5 mice per group. c) Growth curves of E0771 tumors grown in WT and *Bgn* KO mice. Mice were treated with DMSO or 2 mg/kg paclitaxel once every 3 days for a total of 6 treatments. Significance was determined by a one-way ANOVA. n= 4-5 mice per group. d, e) Representative IVIS images of d) metastatic lymph nodes and e) lungs in E0771 tumors of DMSO- or paclitaxel-treated WT and *Bgn* KO mice as described in c).

Discussion

Biglycan has been extensively investigated in cancer cells. Biglycan has bidirectional roles modulating tumor growth and progression (Hu et al., 2014; Sun et al., 2016; Xing et al., 2015). However, the expression and function of stroma biglycan in tumor microenvironment required to be elucidated. In the current study, we found that stromal biglycan inhibition enhanced chemotherapeutic efficacy through normalization of not only the vascular but also the tumor microenvironment, resulting in increased oxygen perfusion and drug delivery (Fig. 11). To our knowledge, this is the first report demonstrating that stromal biglycan mediates destabilization of the tumor microenvironment, suggesting that biglycan can potentially serve as a therapeutic target in combination therapies.

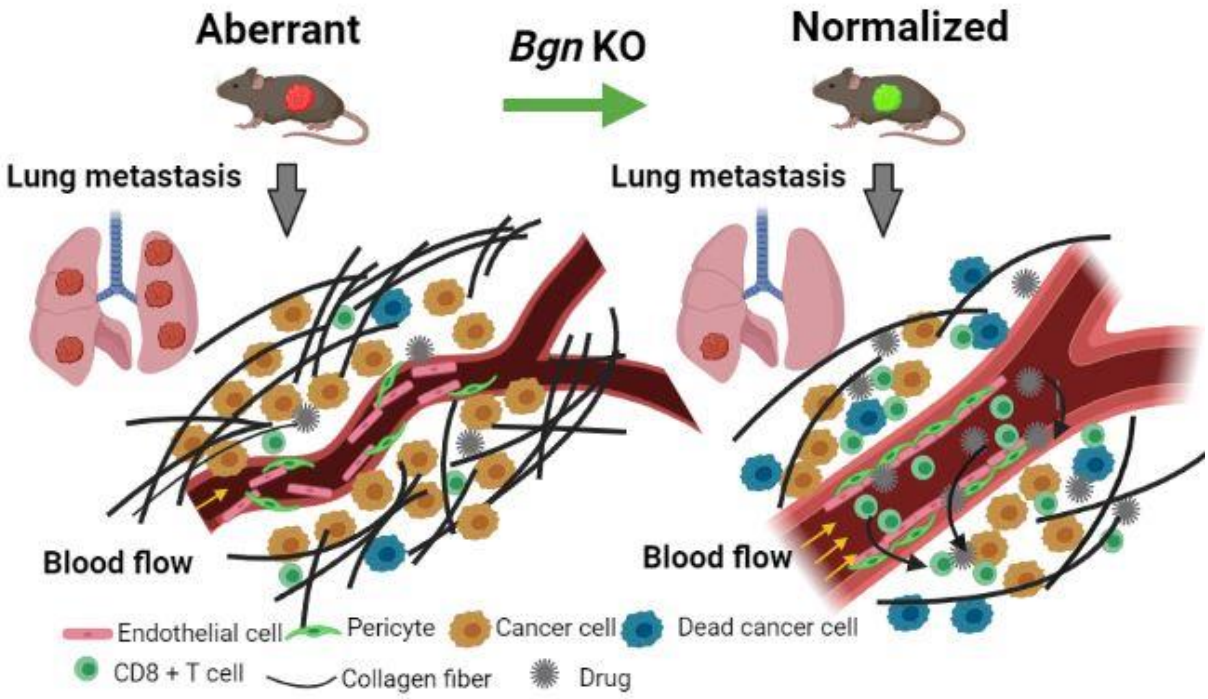

Figure11. Schematic illustrating mechanisms of biglycan modulating tumor microenvironment.

Inactivation of tumor stromal biglycan normalizes tumor vasculature. Biglycan knockout in tumor stroma decreases tumor stiffness and increases the accumulation of CD8+ T cells. Thus, targeting stromal biglycan can facilitate drug delivery in tumors.

Tumor vascular normalization has been shown to enhance tumor oxygenation, reduce cancer progression, and decrease interstitial pressure in the tumor, which consequently enhances drug delivery (Jain, 2013). Treatment with bevacizumab prunes some abnormal vessels and remodels the remaining vessels during the normalization window (Vosseler et al., 2005). However, intrinsic and evasive drug resistance still develops, and the evaluation of the normalization window is still a challenge. There are no validated biomarkers for antiangiogenic agents to maintain normalization of tumor vasculature, and proper molecular diagnostic markers remain to be discovered (Jain, 2013). In the current study, high expression of stromal biglycan associated with a worse outcome in human breast cancers, indicating that tumor stromal biglycan might be involved in tumor progression, further highlighting that biglycan acts as a clinically relevant therapeutic target in breast cancer.

Biglycan has been reported to be expressed in the tumor microenvironment (Maishi et al., 2016; Morimoto et al., 2021; Yamamoto et al., 2012). We previously showed that biglycan is highly expressed in TECs and facilitates cancer metastasis (Maishi et al., 2016; Yamamoto et al., 2012). There might be two main factors regulating biglycan expression in TECs, TGF-β and ROS in tumor microenvironment. In terms of TGF-β, it is reported that the transcription factor of biglycan is SP1, and TGF-β-Smads interacts with SP1 to regulate biglycan expression (Heegaard et al., 2004; Ungefroren and Krull, 1996). Because TGF-β is abundant in the tumor microenvironment (Batlle and Massague, 2019), TGF-β might be one of the factors of biglycan upregulation in TECs. Then we stimulated NECs with TGF-β, the expression of biglycan was increased in NECs. This data indicated that TGF-β can affect biglycan expression in ECs. Another factor reactive oxygen species (ROS) in tumor microenvironment might also affect biglycan in TECs. The tumor microenvironment is exposed to hypoxic condition and nutrient deprivation, which induces ROS accumulation

tumor endothelial cells (Kondoh et al., 2013). We have found that ROS elevated the biglycan expression in ECs. Nuclear factor erythroid 2-related factor 2 (NRF2) protects cells from oxidative and inflammatory stress and mediates ROS response in TECs. ROS inhibited NRF2 expression in TECs and NRF2 inhibited phosphorylation of SMAD2/3, which activates transcription of biglycan (Hojo et al., 2017).

In our study, biglycan was only expressed in tumor blood vessels of mouse breast cancers, and not in normal mammary gland tissue. Furthermore, co-expression analysis by cBioPortal showed that BGN was positively associated with PECAM1 and ANGPT2 expression in human breast cancers. Both PECAM1 and ANGPT2 genes are encoding the angiogenesis related molecules, which means that BGN is involved in regulating angiogenesis. VEGF form a crucial regulatory system for normal and pathological angiogenesis (Ferrara and Davis-Smyth, 1997). In VEGF gene knockout studies, VEGF knockout mice showed embryonic lethality due to multiple defects in vascular structure formation (Ferrara et al., 1996). Unlike VEGF knockout mice, biglycan-deficient mice exhibited no embryonic lethality (Xu et al., 1998). No difference of body weight is observed in *Bgn* KO mice and WT mice (Xu et al., 1998). *Bgn* KO mice have shorter bones with collagen abnormalities compared to WT mice (Ameye et al., 2002). Targeting biglycan may not cause severe damage in normal tissues, and is perhaps unlikely to cause adverse effects. These data indicated that stromal biglycan may be a clinically relevant therapeutic target in breast cancer.

We analyzed the effect of biglycan on breast cancer growth and progression. Biglycan had no effect of proliferation in E0771 cells in vitro. Furthermore, there was no difference of E0771 tumor growth between WT and *Bgn* KO mice. These data indicated that biglycan has no effect on breast cancer cell proliferation and tumor growth. However, it has been reported that biglycan inhibits bladder cancer cell and pancreatic cancer cell proliferation (Niedworok et al., 2013). Biglycan seems to have roles also in tumor growth in some of the tumor type. Our previous data showed that biglycan secreted from TECs can promote tumor cells migration and intravasation through NF-kB and ERK pathways (Maishi et al., 2016). In our previous

report, the numbers of CTCs and the occurrence of lung metastasis were dramatically decreased in mice bearing tumors co-implanted with shBiglycan TECs, compared to the control mice (Maishi et al., 2016). These data indicated that TEC-derived biglycan induces tumor cell metastasize. From the current study, biglycan can enhance tumor angiogenesis in E0771 tumor. Enhanced tumor angiogenesis can facilitate tumor cell metastasis. Biglycan may also lead tumor blood vessels with less pericyte coverage. Tumor blood vessels with less pericyte coverage facilitate tumor cells intravasation. Furthermore, biglycan might be involved in tumor fibrosis. It has been reported that biglycan promotes melanoma tissue stiffness and melanoma cell migration via regulation of integrin-β1 expression (Andrlova et al., 2017). Similarly, our results showed that biglycan enhanced fibrosis in breast cancer tissues, which may mediate tumor metastasis.

In the current study, *Bgn* KO inhibits tumor angiogenesis which indicates biglycan might promote tumor angiogenesis. Previously, we have found that biglycan is an autocrine angiogenic factor of TECs by enhancing TEC migration and tube formation (Yamamoto et al., 2012). In this study, we found that biglycan is associated with Angpt2 which is largely secreted from activated ECs, is directly angiogenic. Tumor vessels were normalized in stroma biglycan deficient tumors, such as increased pericyte coverage and decreased vessel perfusion, leading to a less hypoxic environment and increased drug delivery. Tumor vascular normalization is known to elicit enhanced tumor oxygenation, reduced hemorrhagic necrosis, and decreased interstitial pressure in the tumor, which consequently improves drug delivery (Jain, 2005). Also, biglycan depletion in stroma suppressed tumor fibrosis, consistent with a previous report (Andrlova et al., 2017).Normalization of the tumor microenvironment has also been theorized to enhance drug delivery and the efficiency of chemotherapies (Jain, 2013). Together, these results provide a rationale for the combination therapy of stromal biglycan blockade and the conventional chemotherapeutic agent, paclitaxel. Paclitaxel, widely used to treat breast cancer, both kills and activates tumor cells, thereby increasing chemoresistance and metastasis (Miller et al., 2007). Furthermore, as a DNA damage–inducing drug, paclitaxel may induce severe systematic side effects when used alone or in combination with other drugs, which markedly limits its clinical implication (Luck et al., 2015; Miller et al., 2007). Here we

observed that paclitaxel had a significantly greater effect on tumor growth in biglycan knockout mice compared to WT mice. Therefore, targeting stromal biglycan may enhance the therapeutic potential of chemotherapeutic agents in treating cancers.

We then investigated how inactivation of stromal biglycan induced vascular normalization mechanistically. Pericytes embedded in the basement membrane of blood vessels are important regulators of angiogenesis and vascular stability (Armulik et al., 2005). Pericytes also promote maturation of blood vessels by stabilizing endothelial cells (Greenberg et al., 2008). There are several mechanisms regulating normalizing tumor blood vessels. The blood vessel maturation through improved pericyte coverage and restoration of cell junctions leading to normalization of tumor vasculature. Increased pericyte coverage is mediated by Ang1-Tie2, PDGF-B/PDGFR and BMP signaling. Enhancement of endothelial cell junction can be controlled by increasing VE-cadherin expression (Semenza, 2010). ANGPT2, which is largely secreted from activated ECs, is directly angiogenic, and binding of ANGPT2 to its receptor TIE2 on endothelial cells destabilizes vessels by leading to detachment of pericytes, thereby promoting vascular leakiness (Augustin et al., 2009). Targeting ANGPT2 signaling in tumor vasculature can restore vascular stability and decrease tumor growth and metastasis (Keskin et al., 2015). It has been shown that ANGPT2 is downstream of biglycan signaling in telomerase-immortalized microvascular endothelial cells (Chui et al., 2017). Furthermore, BGN was positively associated with ANGPT2 expression in human breast cancers. We also demonstrated that Angpt2 mRNA is downregulated in stromal biglycan-deficient tumors. Our results suggest that biglycan destabilizes tumor blood vessels by mediating Angpt2 expression. However, biglycan itself indirectly induced Angpt2 expression in endothelial cells. Using IPA, we propose that TNF-α stimulates tumor angiogenesis via suppression of vascular integrity and increased perfusion as a result of biglycan signaling. TNF-α is a major factor in inflammation and cancer progression (Montfort et al., 2019). Furthermore, TNF-α promotes angiogenesis in vivo (Leibovich et al., 1987), and remodels blood vessels during inflammation (Baluk et al., 2009). Targeting TNF-α increases mature blood vessels in rheumatoid arthritis synovium (Izquierdo et al., 2009). As reported, TNF-α specifically induces Ang2 mRNA expression in ECs. Although a high dose of TNF-α on cultured

endothelial cells is inhibitory or apoptotic to endothelial cells (Polunovsky et al., 1994), a low dose of TNF-α indirectly stimulates angiogenesis by inducing production of angiogenic molecules such as VEGF(Angelo and Kurzrock, 2007). Therefore, TNF-α is called an indirect angiogenic factor. Here, Angpt2 produced from endothelial cells in TNF-α stimulated angiogenesis by biglycan. Since TNF-α has been reported to function as an inducer of lymphangiogenesis (Ji et al., 2014), whether imparing TNF-α by stroma biglycan deficiency affecting lymphatic vessel formation needs to be elucidate in future.

Biglycan acts as a DAMP, and here we provided evidence demonstrating that stromal biglycan promotes TNF-α expression in tumor cells through binding to TLR2 or TLR4, and subsequent activation of NF-κB and ERK signaling pathways. Consistent with previous reports (Kim et al., 2000), we also found that increased TNF-α expression led to upregulated Angpt2 mRNA in ECs. These results indicated that stromal biglycan enhances TNF-α expression in tumor cells, and that TNF-α subsequently upregulates Angpt2 expression in ECs, thus destabilizing tumor blood vessels. Furthermore, expression of Mcr1, a M2-like macrophage-associated gene, was decreased in tumor-bearing *Bgn* KO mice (data not shown), which suggests that M2-like macrophages may be altered by stromal biglycan deficiency. M2-like macrophages play a critical role in promoting the formation of an abnormal tumor vascular network and subsequent tumor progression and invasion (Hao et al., 2012). Targeting of M2-like macrophages may also potentially lead to the normalization of tumor vasculature (Rolny et al., 2011). Biglycan has been demonstrated to trigger the synthesis of the macrophage chemoattractant chemokine (C-C motif) ligand CCL2 and CCL5 (Moreth et al., 2014); thus it may be possible that biglycan deficiency modulates tumor vasculature through recruitment of macrophages.

As a DAMP, biglycan induces inflammation and fibrogenesis (Bani-Hani et al., 2009). Biglycan promotes clustering of TLR2/TLR4 with the purinergic P2X7 and P2X4 receptors, which activate NLRP3 (Babelova et al., 2009). The NLRP3 inflammasome triggers secretion of IL-1β and IL-18, which are involved in renal fibrogenesis (Babelova et al., 2009; Jones et

al., 2009). We also observed that biglycan depletion in stroma suppressed tumor fibrosis as well as downregulated collagen I expression. Furthermore, α -SMA + fibroblasts were fewer in biglycan depleted tumors. Biglycan may activate CAFs via upregulating α-SMA expression, thus enhancing fibrosis. Increasing ECM stiffness can enhance cancer progression and metastasis. Biglycan in fibroblasts promotes melanoma invasiveness via increased tissue stiffness, thereby inducing integrin-β1 expression (Andrlova et al., 2017), which is supported by our findings. The ECM in tumors can also impair the function of blood vessels via compression (Martin et al., 2019). Targeting stromal biglycan reduced desmoplasia and overcame vascular compression. Furthermore, destabilizing tumor vasculature and increasing fibrosis can lead to tumor hypoxia (Jain, 2014). We have found that biglycan increased HIF1-α and Glut1 expression in tumor cells. It has been reported that biglycan increased the interaction between NF-kB and the HIF-1a promoter, leading to enhanced promoter activity and increased HIF-1a mRNA levels in endothelial cells (Hu et al., 2016), which is consistent with our findings. HIF1-α is involved in the induction of Glut1 expression (Hayashi et al., 2004). These data indicated that biglycan might be involved in tumor hypoxia response in tumor cells through upregulating HIF1-α and Glut1 expression. Alleviating hypoxia is highly beneficial for improving cancer treatment (Jain, 2014). However, the detailed mechanisms by which biglycan mediates tumor desmoplasia and hypoxia remain unclear.

Triple negative breast cancer (TNBC) constitutes 15% of all breast cancers, and is defined by the lack the expression of hormone receptors and HER2 (Cleator et al., 2007). Recently, TNBC has been approved to be treated with an immune checkpoint inhibitor (ICI) by the Food and Drug Administration (Schmid et al., 2019). Given the moderately favorable immune cell infiltration and response to immunotherapy, the E0771 breast carcinoma model offers significant potential as a preclinical immuno-oncology model. It has been reported that the tumor microenvironment contributes to the induction of lymphocyte anergy, and that altering the microenvironment can restore immune responses against tumors and delay cancer progression (Gajewski et al., 2013). Here, we provide evidence showing that targeting stromal biglycan alters the tumor microenvironment and enhances intratumoral infiltration of CD8+ T cells in a TNBC mouse model (E0771 breast cancer). Our study may lead to a potential

strategy of targeting stroma biglycan to facilitate immune checkpoint inhibitor therapy in human TNBC. However, further precise analysis is required to identify the inhibition of anti-tumor immune responses via modulation of the activation, function, and survival of leukocytes during cancer progression and mechanism whereby other lymphocytes infiltration is not altered even though the tumor microenvironment is improved by stroma biglycan inhibition. Furthermore, as biglycan activates the NF-κB signaling pathway, which is one transcriptional activator of PD-L1 (Wang et al., 2019), we speculate that biglycan may induce PD-L1 expression in tumor cells or tumor stroma cells. Thus, targeting biglycan may achieve superior antitumor effects via multiple parallel pathways.

Conclusion

Summary of the study:

1) Biglycan is highly expressed in tumor stroma.

2) Targeting tumor stromal biglycan normalizes tumor vasculature and inhibits fibrosis.

3) Biglycan knockout promotes CD8+ T-cell infiltration.

4) Deletion of stromal biglycan enhances the efficacy of chemotherapy treatment.

Significance of the study:

The study has been elucidated that targeting stroma biglycan normalizes tumor blood vessels and improves the delivery of chemotherapy agents. Biglycan may be regarded as a promising candidate to potentiate the efficacy of anticancer therapies in breast cancer. Furthermore, a novel target (biglycan) has been discovered to suppress cancer fibrosis and improve immune cell recruitment. In addition, biglycan is expected to enhance the therapeutic effect of immunotherapy and anticancer drugs.

Future research:

Normalization of blood vessels that carry drugs and suppression of fibrosis of cancer tissues are expected to lead to enhanced effects of anticancer drug treatment and immunotherapy. The therapeutic efficacy of targeting biglycan combined with immunotherapy will be discovered. To target cell specific biglycan in tumor, biglycan conditional knock-out mice will be used in the future study. Research is also expected to establish the development of inhibitors targeting biglycan and effective administration methods.

Acknowledgments

Throughout the PhD career in Hokkaido University, I have received a great deal of support and assistance.

I would first like to thank my supervisor, Professor Masaki Murakami of the Department of Molecular Neuroimmunology, who kindly offered me the opportunity to study in Hokkaido University and guided me to the excellent platform to conduct research.

I would also like to thank my mentor, Professor Kyoko Hida of the Department of Vascular Biology and Molecular Pathology. She provided me with the experiment materials and the right direction throughout my studies. She also instructed me how to well behave in the working condition and encouraged me to move forward for creating a limitless research life.

I would like to acknowledge Dr. Nako Maishi during my study. Her insightful comments instructed me to sharpen my thinking and brought my research work to a higher level.

I am deeply grateful to Dr. Yasuhiro Hida for invaluable advice and continuous support in all the time of my academic research.

I would like to offer my special thanks to Marian F. Young who kindly offers *Bgn* KO mice to our lab so that we could continue our research.

To the staff members in our lab, Aya Matsuda, Tetsuya Kitamura, Alam Mohammad Towfik, Yui Umeyama, Yuko Suzuki, Sanae Fukuda, Mika Sasaki and Shogo Baba, I am grateful for their unwavering support to me.

I would like to express my sincere gratitude to my schoolmates and friends, Dorcas A. Annan, Hirofumi Morimoto, Masahiro Morimoto, Masumi Sato, Takuya Tsumita, Jun Furumido, Hironori Tanaka, Erika Akahori, Takashi Niiyama, Hossain Elora, Ahmed Y AlBaloul, Mineyoshi Sato, Hideki Takekawa, Ryo Takeda, Takehiro Chida, Yu Li, Jia Zi Ren Zixiao for their wonderful accompany.

I also express my appreciation to JSPS Grants-in-Aid for Scientific Research, Grants from Japan Agency for Medical Research and Development (AMED) and the Intramural Research Program of the NIH, NIDCR Molecular Biology of Bones and Teeth Section.

Finally, I appreciate all the support I received from my family.

Disclosure of Conflict of Interest

We declare no potential conflicts of interest.

References

Ameye, L., Aria, D., Jepsen, K., Oldberg, A., Xu, T., and Young, M.F. (2002). Abnormal collagen fibrils in tendons of biglycan/fibromodulin-deficient mice lead to gait impairment, ectopic ossification, and osteoarthritis. FASEB J *16*, 673-680.

Amin, D.N., Hida, K., Bielenberg, D.R., and Klagsbrun, M. (2006). Tumor endothelial cells express epidermal growth factor receptor (EGFR) but not ErbB3 and are responsive to EGF and to EGFR kinase inhibitors. Cancer Res *66*, 2173-2180.

Anders, H.J., and Schaefer, L. (2014). Beyond tissue injury-damage-associated molecular patterns, toll-like receptors, and inflammasomes also drive regeneration and fibrosis. J Am Soc Nephrol *25*, 1387-1400.

Andrlova, H., Mastroianni, J., Madl, J., Kern, J.S., Melchinger, W., Dierbach, H., Wernet, F., Follo, M., Technau-Hafsi, K., Has, C., *et al.* (2017). Biglycan expression in the melanoma microenvironment promotes invasiveness via increased tissue stiffness inducing integrin-beta1 expression. Oncotarget *8*, 42901-42916.

Angelo, L.S., and Kurzrock, R. (2007). Vascular endothelial growth factor and its relationship to inflammatory mediators. Clin Cancer Res *13*, 2825-2830.

Aprile, G., Avellini, C., Reni, M., Mazzer, M., Foltran, L., Rossi, D., Cereda, S., Iaiza, E., Fasola, G., and Piga, A. (2013). Biglycan expression and clinical outcome in patients with pancreatic adenocarcinoma. Tumour Biol *34*, 131-137.

Armulik, A., Abramsson, A., and Betsholtz, C. (2005). Endothelial/pericyte interactions. Circ Res *97*, 512-523.

Augustin, H.G., Koh, G.Y., Thurston, G., and Alitalo, K. (2009). Control of vascular morphogenesis and homeostasis through the angiopoietin-Tie system. Nat Rev Mol Cell Biol *10*, 165-177.

Babelova, A., Moreth, K., Tsalastra-Greul, W., Zeng-Brouwers, J., Eickelberg, O., Young, M.F., Bruckner, P., Pfeilschifter, J., Schaefer, R.M., Grone, H.J., *et al.* (2009). Biglycan, a danger signal that activates the NLRP3 inflammasome via toll-like and P2X receptors. J Biol Chem *284*, 24035-24048.

Baluk, P., Yao, L.C., Feng, J., Romano, T., Jung, S.S., Schreiter, J.L., Yan, L., Shealy, D.J., and McDonald, D.M. (2009). TNF-alpha drives remodeling of blood vessels and lymphatics

in sustained airway inflammation in mice. J Clin Invest *119*, 2954-2964.
Bani-Hani, A.H., Leslie, J.A., Asanuma, H., Dinarello, C.A., Campbell, M.T., Meldrum, D.R., Zhang, H., Hile, K., and Meldrum, K.K. (2009). IL-18 neutralization ameliorates obstruction-induced epithelial-mesenchymal transition and renal fibrosis. Kidney Int *76*, 500-511.
Batlle, E., and Massague, J. (2019). Transforming Growth Factor-beta Signaling in Immunity and Cancer. Immunity *50*, 924-940.
Cao, G., O'Brien, C.D., Zhou, Z., Sanders, S.M., Greenbaum, J.N., Makrigiannakis, A., and DeLisser, H.M. (2002). Involvement of human PECAM-1 in angiogenesis and in vitro endothelial cell migration. Am J Physiol Cell Physiol *282*, C1181-1190.
Carmeliet, P., and Jain, R.K. (2011a). Molecular mechanisms and clinical applications of angiogenesis. Nature *473*, 298-307.
Carmeliet, P., and Jain, R.K. (2011b). Principles and mechanisms of vessel normalization for cancer and other angiogenic diseases. Nat Rev Drug Discov *10*, 417-427.
Chauhan, V.P., Martin, J.D., Liu, H., Lacorre, D.A., Jain, S.R., Kozin, S.V., Stylianopoulos, T., Mousa, A.S., Han, X., Adstamongkonkul, P., *et al.* (2013). Angiotensin inhibition enhances drug delivery and potentiates chemotherapy by decompressing tumour blood vessels. Nat Commun *4*, 2516.
Chen, I.X., Chauhan, V.P., Posada, J., Ng, M.R., Wu, M.W., Adstamongkonkul, P., Huang, P., Lindeman, N., Langer, R., and Jain, R.K. (2019). Blocking CXCR4 alleviates desmoplasia, increases T-lymphocyte infiltration, and improves immunotherapy in metastatic breast cancer. Proc Natl Acad Sci U S A *116*, 4558-4566.
Chui, A., Gunatillake, T., Brennecke, S.P., Ignjatovic, V., Monagle, P.T., Whitelock, J.M., van Zanten, D.E., Eijsink, J., Wang, Y., Deane, J., *et al.* (2017). Expression of Biglycan in First Trimester Chorionic Villous Sampling Placental Samples and Altered Function in Telomerase-Immortalized Microvascular Endothelial Cells. Arterioscler Thromb Vasc Biol *37*, 1168-1179.
Ciftciler, R., Ozenirler, S., Yucel, A.A., Cengiz, M., Erkan, G., Buyukdemirci, E., Sonmez, C., and Esendagli, G.Y. (2017). The importance of serum biglycan levels as a fibrosis marker in patients with chronic hepatitis B. J Clin Lab Anal *31*.
Cleator, S., Heller, W., and Coombes, R.C. (2007). Triple-negative breast cancer: therapeutic options. Lancet Oncol *8*, 235-244.

Corsi, A., Xu, T., Chen, X.D., Boyde, A., Liang, J., Mankani, M., Sommer, B., Iozzo, R.V., Eichstetter, I., Robey, P.G., *et al.* (2002). Phenotypic effects of biglycan deficiency are linked to collagen fibril abnormalities, are synergized by decorin deficiency, and mimic Ehlers-Danlos-like changes in bone and other connective tissues. J Bone Miner Res *17*, 1180-1189.
Ferrara, N., Carver-Moore, K., Chen, H., Dowd, M., Lu, L., O'Shea, K.S., Powell-Braxton, L., Hillan, K.J., and Moore, M.W. (1996). Heterozygous embryonic lethality induced by targeted inactivation of the VEGF gene. Nature *380*, 439-442.
Ferrara, N., and Davis-Smyth, T. (1997). The biology of vascular endothelial growth factor. Endocr Rev *18*, 4-25.
Folkman, J. (2002). Role of angiogenesis in tumor growth and metastasis. Semin Oncol *29*, 15-18.
Fu, R., Li, Y., Jiang, N., Ren, B.X., Zang, C.Z., Liu, L.J., Lv, W.C., Li, H.M., Weiss, S., Li, Z.Y., *et al.* (2020). Inactivation of endothelial ZEB1 impedes tumor progression and sensitizes tumors to conventional therapies. J Clin Invest *130*, 1252-1270.
Gajewski, T.F., Schreiber, H., and Fu, Y.X. (2013). Innate and adaptive immune cells in the tumor microenvironment. Nat Immunol *14*, 1014-1022.
Gerstner, E.R., Emblem, K.E., Yen, Y.F., Dietrich, J., Jordan, J.T., Catana, C., Wenchin, K.L., Hooker, J.M., Duda, D.G., Rosen, B.R., *et al.* (2020). Vascular dysfunction promotes regional hypoxia after bevacizumab therapy in recurrent glioblastoma patients. Neurooncol Adv *2*, vdaa157.
Goel, S., Wong, A.H., and Jain, R.K. (2012). Vascular normalization as a therapeutic strategy for malignant and nonmalignant disease. Cold Spring Harb Perspect Med *2*, a006486.
Greenberg, J.I., Shields, D.J., Barillas, S.G., Acevedo, L.M., Murphy, E., Huang, J., Scheppke, L., Stockmann, C., Johnson, R.S., Angle, N., *et al.* (2008). A role for VEGF as a negative regulator of pericyte function and vessel maturation. Nature *456*, 809-813.
Hao, N.B., Lu, M.H., Fan, Y.H., Cao, Y.L., Zhang, Z.R., and Yang, S.M. (2012). Macrophages in tumor microenvironments and the progression of tumors. Clin Dev Immunol *2012*, 948098.
Hara, T., Yoshida, E., Shinkai, Y., Yamamoto, C., Fujiwara, Y., Kumagai, Y., and Kaji, T. (2017). Biglycan Intensifies ALK5-Smad2/3 Signaling by TGF-beta1 and Downregulates Syndecan-4 in Cultured Vascular Endothelial Cells. J Cell Biochem *118*, 1087-1096.

Hashizume, H., Baluk, P., Morikawa, S., McLean, J.W., Thurston, G., Roberge, S., Jain, R.K., and McDonald, D.M. (2000). Openings between defective endothelial cells explain tumor vessel leakiness. Am J Pathol *156*, 1363-1380.

Hayashi, M., Sakata, M., Takeda, T., Yamamoto, T., Okamoto, Y., Sawada, K., Kimura, A., Minekawa, R., Tahara, M., Tasaka, K., *et al.* (2004). Induction of glucose transporter 1 expression through hypoxia-inducible factor 1alpha under hypoxic conditions in trophoblast-derived cells. J Endocrinol *183*, 145-154.

Heegaard, A.M., Xie, Z., Young, M.F., and Nielsen, K.L. (2004). Transforming growth factor beta stimulation of biglycan gene expression is potentially mediated by sp1 binding factors. J Cell Biochem *93*, 463-475.

Hida, K., Hida, Y., Amin, D.N., Flint, A.F., Panigrahy, D., Morton, C.C., and Klagsbrun, M. (2004). Tumor-associated endothelial cells with cytogenetic abnormalities. Cancer Res *64*, 8249-8255.

Hida, K., Hida, Y., and Shindoh, M. (2008). Understanding tumor endothelial cell abnormalities to develop ideal anti-angiogenic therapies. Cancer Sci *99*, 459-466.

Hida, K., Maishi, N., Torii, C., and Hida, Y. (2016). Tumor angiogenesis--characteristics of tumor endothelial cells. Int J Clin Oncol *21*, 206-212.

Hojo, T., Maishi, N., Towfik, A.M., Akiyama, K., Ohga, N., Shindoh, M., Hida, Y., Minowa, K., Fujisawa, T., and Hida, K. (2017). ROS enhance angiogenic properties via regulation of NRF2 in tumor endothelial cells. Oncotarget *8*, 45484-45495.

Hsieh, L.T., Nastase, M.V., Zeng-Brouwers, J., Iozzo, R.V., and Schaefer, L. (2014). Soluble biglycan as a biomarker of inflammatory renal diseases. Int J Biochem Cell Biol *54*, 223-235.

Hu, L., Duan, Y.T., Li, J.F., Su, L.P., Yan, M., Zhu, Z.G., Liu, B.Y., and Yang, Q.M. (2014). Biglycan enhances gastric cancer invasion by activating FAK signaling pathway. Oncotarget *5*, 1885-1896.

Hu, L., Zang, M.D., Wang, H.X., Li, J.F., Su, L.P., Yan, M., Li, C., Yang, Q.M., Liu, B.Y., and Zhu, Z.G. (2016). Biglycan stimulates VEGF expression in endothelial cells by activating the TLR signaling pathway. Mol Oncol *10*, 1473-1484.

Iozzo, R.V. (1999). The biology of the small leucine-rich proteoglycans. Functional network of interactive proteins. J Biol Chem *274*, 18843-18846.

Itatani, Y., Kawada, K., Yamamoto, T., and Sakai, Y. (2018). Resistance to Anti-Angiogenic

Therapy in Cancer-Alterations to Anti-VEGF Pathway. Int J Mol Sci *19*.
Izquierdo, E., Canete, J.D., Celis, R., Santiago, B., Usategui, A., Sanmarti, R., Del Rey, M.J., and Pablos, J.L. (2009). Immature blood vessels in rheumatoid synovium are selectively depleted in response to anti-TNF therapy. PLoS One *4*, e8131.
Jain, R.K. (2005). Normalization of tumor vasculature: an emerging concept in antiangiogenic therapy. Science *307*, 58-62.
Jain, R.K. (2013). Normalizing tumor microenvironment to treat cancer: bench to bedside to biomarkers. J Clin Oncol *31*, 2205-2218.
Jain, R.K. (2014). Antiangiogenesis strategies revisited: from starving tumors to alleviating hypoxia. Cancer Cell *26*, 605-622.
Jain, R.K., Tong, R.T., and Munn, L.L. (2007). Effect of vascular normalization by antiangiogenic therapy on interstitial hypertension, peritumor edema, and lymphatic metastasis: insights from a mathematical model. Cancer Res *67*, 2729-2735.
Ji, H., Cao, R., Yang, Y., Zhang, Y., Iwamoto, H., Lim, S., Nakamura, M., Andersson, P., Wang, J., Sun, Y., *et al.* (2014). TNFR1 mediates TNF-alpha-induced tumour lymphangiogenesis and metastasis by modulating VEGF-C-VEGFR3 signalling. Nat Commun *5*, 4944.
Jones, L.K., O'Sullivan, K.M., Semple, T., Kuligowski, M.P., Fukami, K., Ma, F.Y., Nikolic-Paterson, D.J., Holdsworth, S.R., and Kitching, A.R. (2009). IL-1RI deficiency ameliorates early experimental renal interstitial fibrosis. Nephrol Dial Transplant *24*, 3024-3032.
Keskin, D., Kim, J., Cooke, V.G., Wu, C.C., Sugimoto, H., Gu, C., De Palma, M., Kalluri, R., and LeBleu, V.S. (2015). Targeting vascular pericytes in hypoxic tumors increases lung metastasis via angiopoietin-2. Cell Rep *10*, 1066-1081.
Kikuchi, H., Maishi, N., Annan, D.A., Alam, M.T., Dawood, R.I.H., Sato, M., Morimoto, M., Takeda, R., Ishizuka, K., Matsumoto, R., *et al.* (2020). Chemotherapy-Induced IL8 Upregulates MDR1/ABCB1 in Tumor Blood Vessels and Results in Unfavorable Outcome. Cancer Res *80*, 2996-3008.
Kim, I., Kim, J.H., Ryu, Y.S., Liu, M., and Koh, G.Y. (2000). Tumor necrosis factor-alpha upregulates angiopoietin-2 in human umbilical vein endothelial cells. Biochem Biophys Res Commun *269*, 361-365.
Kondoh, M., Ohga, N., Akiyama, K., Hida, Y., Maishi, N., Towfik, A.M., Inoue, N., Shindoh,

M., and Hida, K. (2013). Hypoxia-induced reactive oxygen species cause chromosomal abnormalities in endothelial cells in the tumor microenvironment. PLoS One *8*, e80349.
Leibovich, S.J., Polverini, P.J., Shepard, H.M., Wiseman, D.M., Shively, V., and Nuseir, N. (1987). Macrophage-induced angiogenesis is mediated by tumour necrosis factor-alpha. Nature *329*, 630-632.
Liu, Y., Li, W., Li, X., Tai, Y., Lu, Q., Yang, N., and Jiang, J. (2014). Expression and significance of biglycan in endometrial cancer. Arch Gynecol Obstet *289*, 649-655.
Luck, H.J., Lubbe, K., Reinisch, M., Maass, N., Feisel-Schwickardi, G., Tome, O., Janni, W., Aydogdu, M., Neunhoffer, T., Ober, A., *et al.* (2015). Phase III study on efficacy of taxanes plus bevacizumab with or without capecitabine as first-line chemotherapy in metastatic breast cancer. Breast Cancer Res Treat *149*, 141-149.
Maishi, N., Ohba, Y., Akiyama, K., Ohga, N., Hamada, J., Nagao-Kitamoto, H., Alam, M.T., Yamamoto, K., Kawamoto, T., Inoue, N., *et al.* (2016). Tumour endothelial cells in high metastatic tumours promote metastasis via epigenetic dysregulation of biglycan. Sci Rep *6*, 28039.
Martin, J.D., Seano, G., and Jain, R.K. (2019). Normalizing Function of Tumor Vessels: Progress, Opportunities, and Challenges. Annu Rev Physiol *81*, 505-534.
Matsuda, K., Ohga, N., Hida, Y., Muraki, C., Tsuchiya, K., Kurosu, T., Akino, T., Shih, S.C., Totsuka, Y., Klagsbrun, M., *et al.* (2010). Isolated tumor endothelial cells maintain specific character during long-term culture. Biochem Biophys Res Commun *394*, 947-954.
Miller, K., Wang, M., Gralow, J., Dickler, M., Cobleigh, M., Perez, E.A., Shenkier, T., Cella, D., and Davidson, N.E. (2007). Paclitaxel plus bevacizumab versus paclitaxel alone for metastatic breast cancer. N Engl J Med *357*, 2666-2676.
Montfort, A., Colacios, C., Levade, T., Andrieu-Abadie, N., Meyer, N., and Segui, B. (2019). The TNF Paradox in Cancer Progression and Immunotherapy. Front Immunol *10*, 1818.
Moreth, K., Brodbeck, R., Babelova, A., Gretz, N., Spieker, T., Zeng-Brouwers, J., Pfeilschifter, J., Young, M.F., Schaefer, R.M., and Schaefer, L. (2010). The proteoglycan biglycan regulates expression of the B cell chemoattractant CXCL13 and aggravates murine lupus nephritis. J Clin Invest *120*, 4251-4272.
Moreth, K., Frey, H., Hubo, M., Zeng-Brouwers, J., Nastase, M.V., Hsieh, L.T., Haceni, R., Pfeilschifter, J., Iozzo, R.V., and Schaefer, L. (2014). Biglycan-triggered TLR-2- and TLR-4-

signaling exacerbates the pathophysiology of ischemic acute kidney injury. Matrix Biol *35*, 143-151.
Morimoto, H., Hida, Y., Maishi, N., Nishihara, H., Hatanaka, Y., Li, C., Matsuno, Y., Nakamura, T., Hirano, S., and Hida, K. (2021). Biglycan, tumor endothelial cell secreting proteoglycan, as possible biomarker for lung cancer. Thorac Cancer *12*, 1347-1357.
Nagy, J.A., Chang, S.H., Dvorak, A.M., and Dvorak, H.F. (2009). Why are tumour blood vessels abnormal and why is it important to know? Br J Cancer *100*, 865-869.
Nagy, J.A., Feng, D., Vasile, E., Wong, W.H., Shih, S.C., Dvorak, A.M., and Dvorak, H.F. (2006). Permeability properties of tumor surrogate blood vessels induced by VEGF-A. Lab Invest *86*, 767-780.
Niedworok, C., Rock, K., Kretschmer, I., Freudenberger, T., Nagy, N., Szarvas, T., Vom Dorp, F., Reis, H., Rubben, H., and Fischer, J.W. (2013). Inhibitory role of the small leucine-rich proteoglycan biglycan in bladder cancer. PLoS One *8*, e80084.
Ohga, N., Hida, K., Hida, Y., Muraki, C., Tsuchiya, K., Matsuda, K., Ohiro, Y., Totsuka, Y., and Shindoh, M. (2009). Inhibitory effects of epigallocatechin-3 gallate, a polyphenol in green tea, on tumor-associated endothelial cells and endothelial progenitor cells. Cancer Sci *100*, 1963-1970.
Papetti, M., and Herman, I.M. (2002). Mechanisms of normal and tumor-derived angiogenesis. Am J Physiol Cell Physiol *282*, C947-970.
Polunovsky, V.A., Wendt, C.H., Ingbar, D.H., Peterson, M.S., and Bitterman, P.B. (1994). Induction of endothelial cell apoptosis by TNF alpha: modulation by inhibitors of protein synthesis. Exp Cell Res *214*, 584-594.
Poluzzi, C., Nastase, M.V., Zeng-Brouwers, J., Roedig, H., Hsieh, L.T., Michaelis, J.B., Buhl, E.M., Rezende, F., Manavski, Y., Bleich, A., *et al.* (2019). Biglycan evokes autophagy in macrophages via a novel CD44/Toll-like receptor 4 signaling axis in ischemia/reperfusion injury. Kidney Int *95*, 540-562.
Rivera, L.B., and Bergers, G. (2015). CANCER. Tumor angiogenesis, from foe to friend. Science *349*, 694-695.
Roedig, H., Nastase, M.V., Frey, H., Moreth, K., Zeng-Brouwers, J., Poluzzi, C., Hsieh, L.T., Brandts, C., Fulda, S., Wygrecka, M., *et al.* (2019). Biglycan is a new high-affinity ligand for CD14 in macrophages. Matrix Biol *77*, 4-22.

Rolny, C., Mazzone, M., Tugues, S., Laoui, D., Johansson, I., Coulon, C., Squadrito, M.L., Segura, I., Li, X., Knevels, E., *et al.* (2011). HRG inhibits tumor growth and metastasis by inducing macrophage polarization and vessel normalization through downregulation of PlGF. Cancer Cell *19*, 31-44.

Sahai, E., Astsaturov, I., Cukierman, E., DeNardo, D.G., Egeblad, M., Evans, R.M., Fearon, D., Greten, F.R., Hingorani, S.R., Hunter, T., *et al.* (2020). A framework for advancing our understanding of cancer-associated fibroblasts. Nat Rev Cancer *20*, 174-186.

Schaefer, L., Babelova, A., Kiss, E., Hausser, H.J., Baliova, M., Krzyzankova, M., Marsche, G., Young, M.F., Mihalik, D., Gotte, M., *et al.* (2005). The matrix component biglycan is proinflammatory and signals through Toll-like receptors 4 and 2 in macrophages. J Clin Invest *115*, 2223-2233.

Schmid, P., Chui, S.Y., and Emens, L.A. (2019). Atezolizumab and Nab-Paclitaxel in Advanced Triple-Negative Breast Cancer. Reply. N Engl J Med *380*, 987-988.

Schonherr, E., Witsch-Prehm, P., Harrach, B., Robenek, H., Rauterberg, J., and Kresse, H. (1995). Interaction of biglycan with type I collagen. J Biol Chem *270*, 2776-2783.

Schrimpf, C., Teebken, O.E., Wilhelmi, M., and Duffield, J.S. (2014). The role of pericyte detachment in vascular rarefaction. J Vasc Res *51*, 247-258.

Schulz, G.B., Grimm, T., Sers, C., Riemer, P., Elmasry, M., Kirchner, T., Stief, C.G., Karl, A., and Horst, D. (2019). Prognostic value and association with epithelial-mesenchymal transition and molecular subtypes of the proteoglycan biglycan in advanced bladder cancer. Urol Oncol *37*, 530 e539-530 e518.

Semenza, G.L. (2010). Defining the role of hypoxia-inducible factor 1 in cancer biology and therapeutics. Oncogene *29*, 625-634.

Shimizu-Hirota, R., Sasamura, H., Kuroda, M., Kobayashi, E., Hayashi, M., and Saruta, T. (2004). Extracellular matrix glycoprotein biglycan enhances vascular smooth muscle cell proliferation and migration. Circ Res *94*, 1067-1074.

Shrimali, R.K., Yu, Z., Theoret, M.R., Chinnasamy, D., Restifo, N.P., and Rosenberg, S.A. (2010). Antiangiogenic agents can increase lymphocyte infiltration into tumor and enhance the effectiveness of adoptive immunotherapy of cancer. Cancer Res *70*, 6171-6180.

Stylianopoulos, T., Munn, L.L., and Jain, R.K. (2018). Reengineering the Tumor Vasculature: Improving Drug Delivery and Efficacy. Trends Cancer *4*, 258-259.

Sun, H., Wang, X., Zhang, Y., Che, X., Liu, Z., Zhang, L., Qiu, C., Lv, Q., and Jiang, J. (2016). Biglycan enhances the ability of migration and invasion in endometrial cancer. Arch Gynecol Obstet *293*, 429-438.

Sung, H., Ferlay, J., Siegel, R.L., Laversanne, M., Soerjomataram, I., Jemal, A., and Bray, F. (2021). Global Cancer Statistics 2020: GLOBOCAN Estimates of Incidence and Mortality Worldwide for 36 Cancers in 185 Countries. CA Cancer J Clin *71*, 209-249.

Tolaney, S.M., Boucher, Y., Duda, D.G., Martin, J.D., Seano, G., Ancukiewicz, M., Barry, W.T., Goel, S., Lahdenrata, J., Isakoff, S.J., *et al.* (2015). Role of vascular density and normalization in response to neoadjuvant bevacizumab and chemotherapy in breast cancer patients. Proc Natl Acad Sci U S A *112*, 14325-14330.

Tufvesson, E., and Westergren-Thorsson, G. (2003). Biglycan and decorin induce morphological and cytoskeletal changes involving signalling by the small GTPases RhoA and Rac1 resulting in lung fibroblast migration. J Cell Sci *116*, 4857-4864.

Ueda, S., Saeki, T., Osaki, A., Yamane, T., and Kuji, I. (2017). Bevacizumab Induces Acute Hypoxia and Cancer Progression in Patients with Refractory Breast Cancer: Multimodal Functional Imaging and Multiplex Cytokine Analysis. Clin Cancer Res *23*, 5769-5778.

Ungefroren, H., and Krull, N.B. (1996). Transcriptional regulation of the human biglycan gene. J Biol Chem *271*, 15787-15795.

Vosseler, S., Mirancea, N., Bohlen, P., Mueller, M.M., and Fusenig, N.E. (2005). Angiogenesis inhibition by vascular endothelial growth factor receptor-2 blockade reduces stromal matrix metalloproteinase expression, normalizes stromal tissue, and reverts epithelial tumor phenotype in surface heterotransplants. Cancer Res *65*, 1294-1305.

Wang, W., Chapman, N.M., Zhang, B., Li, M., Fan, M., Laribee, R.N., Zaidi, M.R., Pfeffer, L.M., Chi, H., and Wu, Z.H. (2019). Upregulation of PD-L1 via HMGB1-Activated IRF3 and NF-kappaB Contributes to UV Radiation-Induced Immune Suppression. Cancer Res *79*, 2909-2922.

Welt, A., Marschner, N., Lerchenmueller, C., Decker, T., Steffens, C.C., Koehler, A., Depenbusch, R., Busies, S., and Hegewisch-Becker, S. (2016). Capecitabine and bevacizumab with or without vinorelbine in first-line treatment of HER2/neu-negative metastatic or locally advanced breast cancer: final efficacy and safety data of the randomised, open-label superiority phase 3 CARIN trial. Breast Cancer Res Treat *156*, 97-107.

Xing, X., Gu, X., Ma, T., and Ye, H. (2015). Biglycan up-regulated vascular endothelial growth factor (VEGF) expression and promoted angiogenesis in colon cancer. Tumour Biol *36*, 1773-1780.

Xu, L., Duda, D.G., di Tomaso, E., Ancukiewicz, M., Chung, D.C., Lauwers, G.Y., Samuel, R., Shellito, P., Czito, B.G., Lin, P.C., *et al.* (2009). Direct evidence that bevacizumab, an anti-VEGF antibody, up-regulates SDF1alpha, CXCR4, CXCL6, and neuropilin 1 in tumors from patients with rectal cancer. Cancer Res *69*, 7905-7910.

Xu, T., Bianco, P., Fisher, L.W., Longenecker, G., Smith, E., Goldstein, S., Bonadio, J., Boskey, A., Heegaard, A.M., Sommer, B., *et al.* (1998). Targeted disruption of the biglycan gene leads to an osteoporosis-like phenotype in mice. Nat Genet *20*, 78-82.

Yamamoto, K., Ohga, N., Hida, Y., Maishi, N., Kawamoto, T., Kitayama, K., Akiyama, K., Osawa, T., Kondoh, M., Matsuda, K., *et al.* (2012). Biglycan is a specific marker and an autocrine angiogenic factor of tumour endothelial cells. Br J Cancer *106*, 1214-1223.